Spin-Peierls order parameter and antiferromagnetism in the dimerized and incommensurate phases of Zn-doped CuGeO$_3$

B. Büchner, T. Lorenz, R. Walter, and H. Kierspel

II. Physikalisches Institut, Universität zu Köln, Zülpicher Straße 77, D-50937 Köln, Germany

A. Revcolevschi and G. Dhalenne

Laboratoire de Chimie des Solides, Université Paris-Sud, 91405 Orsay Cédex, France

(Received 6 August 1998)

Measurements of the thermal-expansion coefficient, the magnetostriction, and the specific heat of Zn-doped CuGeO$_3$ single crystals ($x \leqslant 3.3\%$) in magnetic fields up to 16 T are presented. Measuring the lattice constant as a function of temperature, magnetic field, and doping concentration allows us to determine the concentration and field dependence of the averaged spin-Peierls order parameter. A strong reduction upon doping is observed and interpreted in terms of solitonlike defects of the dimerization. From these data the relationship between the averaged spin-Peierls order parameter in doped CuGeO$_3$ and the transition temperature T_{SP} is extracted. The specific heat at low temperatures is dominated by doping induced low-energy excitations. The temperature and field dependence of the corresponding contribution to the specific heat is discussed in a model with random magnetic exchange constants. Studying the thermodynamic properties as a function of an external field, we determine the magnetic field vs temperature phase diagrams of Cu$_{1-x}$Zn$_x$GeO$_3$. Several systematic changes upon doping are revealed. In particular, we find a strong enhancement of disorder in doped CuGeO$_3$, when entering the incommensurate phase with increasing field which we attribute to an additional randomness of the order-parameter phase. Moreover, this field-induced phase transition between dimerized and incommensurate phases is accompanied by a pronounced increase of the antiferromagnetic ordering temperature T_N. A phenomenological description assuming a coupling between the spin-Peierls and the antiferromagnetic order parameters is presented, which allows us to interpret simultaneously both field and concentration dependences of T_N. [S0163-1829(99)08305-8]

I. INTRODUCTION

The discovery of the inorganic spin-Peierls (SP) compound CuGeO$_3$ (Ref. 1) opened the possibility of studying the influence of doping on this magnetoelastic transition, occurring in spin-half antiferromagnetic chains.[2,3] During the last years several surprising features are revealed from the intensive studies of the concentration vs temperature $[(x,T)]$ phase diagrams.[4–17] While the spin-Peierls transition (SPT) is drastically suppressed already by a small amount of dopants, a long-range antiferromagnetic (AFM) order develops. The Néel temperature (T_N) initially increases upon doping and, more surprisingly, the AFM and the SP state coexist in a considerably large range of doping.[18,11,12,19,13,20,15] This is observed for various dopants, such as Zn, Mg, Ni at the Cu site and also by replacing a small amount of Ge by Si. Indeed, an universal (x,T) phase diagram for all dopants is observed, when taking into account a different scale on the concentration axis for CuGe$_{1-y}$Si$_y$O$_3$.[14]

Triggered by the experimental observations, several theoretical studies of doped SP systems have been performed.[21–31] One important result of these studies was the explanation of coexisting SP and AFM phases, which mutually exclude each other in a homogeneous system.[32] It is argued that the dopants cause solitonlike defects in the alternating structural deformation of the lattice. In a homogeneous SP system this structural dimerization implies alternating magnetic exchanges below the SP transition temperature T_{SP} which lead to a nonmagnetic singlet state[33,34,2]. However, AFM correlations develop in inhomogeneous systems, since the solitonlike defects carry a spin-1/2, and therefore a long-range Néel state can occur below T_{SP}.

The response to an external magnetic field is one of the characteristic features of SP systems.[2,33,35–37] Due to the additional Zeeman energy, the nonmagnetic dimerized (D) phase is destabilized in comparison with a magnetic high-field phase. Instead of a doubling of the unit cell present in the D phase, the high-field phase is characterized by an incommensurate (I) modulation of the uniform (U) high-temperature structure. Similar to the case of doping, there are nodes of the order parameter in the I phase, whose distance decreases with increasing H. Some experimental observations indicate that the I phase should be described in terms of a regular lattice of solitons for both CuGeO$_3$ (Refs. 38–40), as well as, the organic SP compound TTF-AuBDT.[42] Each soliton carries a spin-1/2, leading to the finite magnetization. More recently, it was shown that this soliton description of the I phase is only possible close to the field induced D/I transition at $H_{D/I}$, whereas at higher fields a simple sinusoidal modulation is present.[41] Besides the stabilization of the I phase, the external field also reduces T_{SP}. Theoretical studies predict a universal (H,T) phase diagram in SP systems, i.e., the phase boundaries are determined by $T_{SP}(H=0)$ alone.[35,33,36,37,2] The experimentally observed $T_{SP}(H)$ in CuGeO$_3$ is in fair agreement with these predictions (see, e.g., Refs. 43,3). There are, however, significant deviations for the U/I transition at high magnetic fields.[41]

Measurements of the thermodynamic properties specific heat (C), thermal expansion (α), and magnetostriction allow for a detailed study of the (H,T) phase diagram.[43,44,41,45–47] Not only the phase boundaries, but also characteristic properties of phase transitions are revealed by these data, such as, e.g., fluctuations and hystereses.[48,49,43,44] Moreover, the specific heat and the thermal expansion contain information on the magnetic excitations and on the structural deformations, respectively, which are both important in the case of a SPT.[50,43,41,51] Investigations on pure CuGeO$_3$ reveal that the specific heat is mainly determined by the magnetic excitations showing a spin gap (Δ) in the D phase,[52,48,50,51] whereas measurements of α and the magnetostriction allow us to study in detail the temperature and field dependence of the SP order parameter, i.e., the structural distortion.[49,43,44,41]

Some measurements of the above-mentioned thermodynamic properties have also been reported for doped CuGeO$_3$,[53,45,46] focusing on quite different aspects. It was shown that Zn and Si doping drastically affects the behavior of both C and α at T_{SP} and in the SP phase.[53] One conclusion of this study was the increase of the pressure derivative of T_{SP} upon doping. This was later confirmed by measurements at finite pressures[54] and explained qualitatively by a pressure-dependent frustration of the quasi-one-dimensional AFM exchange,[55,51] leading to a pressure-dependent soliton width. A second focus was the study of the field dependence of the AFM state in Si-doped CuGeO$_3$ from measurements of α and C.[45,46] As a main result of these investigations, indications for an unusual AFM state in the dimerized phase of a Si-doped CuGeO$_3$ crystal are derived.[45,46]

The properties of doped CuGeO$_3$ in high magnetic fields have also been studied by other experimental techniques, such as ultrasound measurements,[56–58] magnetization measurements,[59] and diffraction techniques.[40,60] The phase boundaries expected for a SP compound have been found in the doped compounds, too. There are, however, some significant differences in the reported (H,T) phase diagrams (see, e.g.. Refs. 46,56).

In this paper we present a comprehensive study of the specific heat, the thermal expansion, and the magnetostriction measured on a series of Cu$_{1-x}$Zn$_x$GeO$_3$ single crystals in magnetic fields up to 16 T. We focus on the concentration and field dependence of the averaged SP order-parameter square $\langle A^2 \rangle$ as extracted from the temperature, concentration, and field dependences of α and the magnetostriction. A strong reduction of $\langle A^2 \rangle$ upon doping is revealed which is explained in terms of a soliton picture. The (H,T) phase diagrams as well as their systematic change upon doping are shown and discussed. In particular, from our data we extract relationships between $\langle A^2 \rangle$ on the one hand, and the transition temperatures T_{SP} and T_N on the other hand. Moreover, we present an analysis of the specific heat, revealing both signatures of the singlet triplet excitations and a doping-induced contribution dominating at low temperatures.

The paper is organized as follows. After a short description of the experiments we show and analyze the doping dependence of the SP order parameter in zero magnetic field. Focusing on one crystal doped with an intermediate doping of $x=1.4\%$ Zn, we present the results of our α, C and mag-

netostriction measurements in external fields in Sec. IV. The (H,T) phase diagrams of all studied samples are shown and compared in Sec. V. A detailed discussion of the structural distortion of the I phase in doped CuGeO$_3$ is presented in Sec. VI. In this section we will, in addition, discuss the coupling between AFM order and the SP order parameter. Finally, our main conclusions are summarized in Sec. VII.

II. EXPERIMENT

The Cu$_{1-x}$Zn$_x$GeO$_3$ single crystals with a typical mass of $\simeq 500$ mg used in the present study are cut from larger crystals grown from the melt by a floating-zone technique.[61,62] Measurements are presented for Zn concentrations of 0.66%, 1.4% and 3.3% and compared to the findings in pure CuGeO$_3$. The stoichiometry of the Zn-doped crystals was determined using inductively-coupled plasma emission spectroscopy. The obtained Zn contents are smaller ($\sim 25\%$) than the nominal compositions. Crystals prepared in the same way or even other pieces of the same crystals have been used for several studies reported in the literature (e.g., Refs. 14,58,57,54,53). For comparison we will also show and/or refer to measurements on Si-doped crystals, prepared in the same way. While there is not much controversy concerning the findings on different Cu$_{1-x}$Zn$_x$GeO$_3$ crystals, the reported (y,T) phase diagrams markedly differ for CuGe$_{1-y}$Si$_y$O$_3$.[4,6,63,46,20,15] The properties of our Si-doped crystals are discussed in detail in Refs. 4,18,6,14. In particular, it is shown there that the phase diagrams of Cu$_{1-x}$Zn$_x$GeO$_3$ and CuGe$_{1-y}$Si$_y$O$_3$ are identical besides an about three times larger influence of the Si content on both the SPT and the AFM order. Note that for the Si-doped crystals used in Refs. 45,46,20,15 the corresponding factor is much smaller (between 1.5 and 2, see also the discussion in Refs. 20,15). In the context of this paper, we are mainly interested in the magnetic-field dependences at fixed disorder strength and their systematic changes. Therefore we introduce an effective doping x_{eff} in the case of Si doping in order to allow a direct comparison with the observations in Cu$_{1-x}$Zn$_x$GeO$_3$. This effective doping is estimated by comparing the measured T_{SP} and/or T_N with the findings in Cu$_{1-x}$Zn$_x$GeO$_3$, i.e., for our CuGe$_{1-y}$Si$_y$O$_3$ crystals $x_{eff} \simeq 3y$.

For our measurements of the linear coefficients of the thermal expansion $\alpha=(1/L)\Delta L/\Delta T$ (L is the length of the sample) at fixed magnetic field as well as for the measurements of the magnetostriction, i.e., the field-induced length changes $(1/L)\Delta L(H)$ at fixed temperature, a high-resolution capacitance dilatometer described in Ref. 43 was used. Measuring these macroscopic length changes on a single crystal in a given direction allows to extract the normalized temperature and field dependence of the corresponding lattice constant with very high resolution.[43] Even the small effects due to the magnetoelastic coupling in the U phase are clearly resolved from both the thermal expansion[49] and the magnetostriction.[55,44]

In all reported measurements, the magnetic field was applied parallel to the measuring direction. Data were recorded
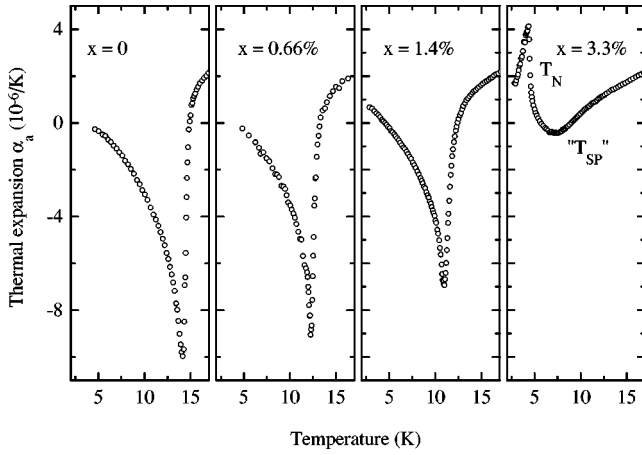
FIG. 1. Thermal-expansion coefficient along the a direction for $Cu_{1-x}Zn_xGeO_3$ crystals with different Zn contents given in the figure.
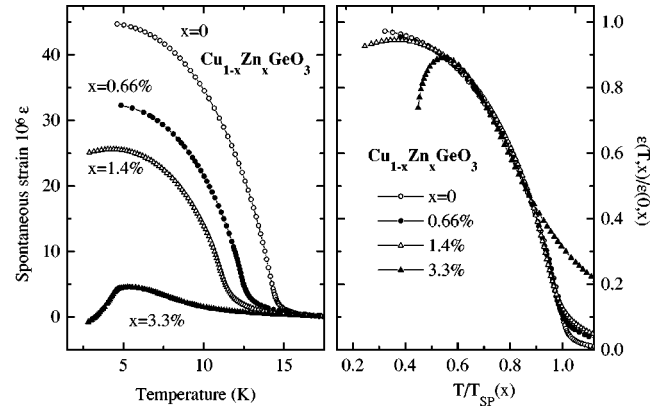

FIG. 2. Left: Spontaneous strains of the lattice constant a as obtained from the data in Fig. 1 after subtraction of a concentration independent extrapolation of the high-temperature behavior. Right: Same data, plotted in reduced scales.

for all three lattice directions of the orthorhombic structure. In all cases the anisotropy is similar to that found in pure $CuGeO_3$.[49,55] In particular, there is no qualitative difference between the findings parallel (c) and perpendicular to the AFM chains. Here we will mainly present results along the a axis, i.e., α_a and $\Delta a(H)/a$, which we have also shown in detail for pure $CuGeO_3$ in previous publications.[43,41] Some representative data for the other lattice and field orientations are shown in addition, in order to demonstrate the similarity.

The specific heat of the crystal doped with 1.4% Zn was measured in fields ranging between 0 and 16 T applied along the c direction, using a quasiadiabatic heat pulse method. The relative resolution (scatter of the data) of the calorimeter is better than $\simeq 0.5\%$, whereas the error in the absolute values is slightly larger ($\simeq 1\%$).

III. ZERO-FIELD DATA: DOPING-INDUCED SOLITONS

In Fig. 1 we show the thermal expansion of the lattice constant a for pure $CuGeO_3$ and three Zn-doped crystals. The drastic influence of the Zn doping on the SP transition is obvious. The transition temperature reduces upon doping with a rate of about $(\Delta T_{SP}/\Delta x)/T_{SP}(0) \simeq 15$ in agreement with other observations in $Cu_{1-x}Zn_xGeO_3$.[64,5,14] Besides this well-known decrease of T_{SP}, there is a drastic influence of the Zn doping on the anomalies of α_a. For small doping amounts, i.e., $x = 0.66\%$ and $x = 1.4\%$, α_a still shows a well-defined phase transition. The anomaly size, however, strongly decreases with increasing Zn concentration. For the sample with the largest concentration ($x = 3.3\%$), the SPT is hardly visible. A closer inspection of α_a, as well as the field dependence shown below, clearly reveals a SP-like phase for this sample, too. However, a well-defined transition temperature in the thermodynamic sense does not exist anymore. Instead the anomalous decrease of α_a occurs in a wide temperature range.

Whereas the anomaly of α_a at T_{SP} is reduced, a second anomaly of the thermal expansion develops at low temperatures, which is connected with the transition to long-range AFM order.[53] In the sample with $x = 3.3\%$ this transition at $T_N \simeq 4.5$ K is apparent. Precursors of this second transition are also visible for the $x = 1.4\%$ sample (see below). Note

that the large anomaly of α_a at T_N signals a pronounced coupling between the AFM order and lattice strains.

In order to analyze the strong decrease of the anomaly of α_a at the SPT upon doping, we consider the spontaneous strains ϵ, i.e., the differences of the lattice constants in the D and U phases. These are obtained by integration of the difference between measured and extrapolated α_a as shown, e.g., in Refs. 49,50,43,53,41. Since our data do not show any significant change of α_a as a function of x above 14 K, we use the same background for all samples. The extracted ϵ are displayed in the left part of Fig. 2. It is apparent that ϵ at low temperatures shows a similar reduction due to Zn doping as the anomalies of α_a at T_{SP}.[65]

As has been pointed out previously[49,43,41] ϵ is closely related to the SP order parameter, i.e., the alternating displacements $A = (-1)^l A_0$ of the atoms in the D phase. Both a Landau expansion of the free energy as well as a comparison with neutron-diffraction data reveal that ϵ is proportional to the square of the structural dimerization, i.e., $\epsilon(T,H) \propto A^2(T,H)$.[43] Note that such a strain order parameter coupling is quite usual at structural phase transitions, signaling, e.g., a small anharmonicity of the lattice. The simple scaling between ϵ and A^2 has been used to study in detail field and temperature dependence of the SP order parameter from high-resolution dilatometry.[49,50,43,41]

As long as a well-defined SP transition is present, Zn doping does not change the temperature dependence of ϵ significantly. This is displayed in the right part of Fig. 2, where we plot ϵ vs T in reduced scales. The same curve is obtained for the samples with $x \lesssim 1.4\%$. This scaling behavior is also found for the spontaneous strains of the incommensurate high-field phase.[50,43,41,66] Doping-induced defects (for small x) as well as the nodes of the order parameter in the high-field phase do not alter the temperature dependence of ϵ. Plotting the strain data for $x = 3.3\%$ in the same way, does, however, not lead to a meaningful result. The anomaly is extremely broad and, as a consequence, the curvature of the ϵ vs T curve is different for temperatures above about 6 K. Moreover, at low temperature the data for $x = 3.3\%$ are dominated by the anomaly at the AFM order.

For a homogeneous structural distortion in the dimerized phase, ϵ scales with the SP order-parameter square as men-

tioned above. However, a homogeneous dimerization is very unlikely in the case of doped compounds, since the Zn ions cut the antiferromagnetic chains into segments. Theoretical treatments, which are supported by recent μSR studies,[19] show that due to these defects, local AFM correlations develop. Simultaneously, the SP order parameter is locally suppressed. Solitonlike defects of the dimerization occur.[21–31] Thus the dimerization amplitude A varies spatially. The macroscopic quantity ϵ does not reveal any direct information on this variation, since it measures the spatial average $\langle A^2 \rangle$. However, theoretical predictions for the defect structure can be easily compared to the measurements of $\langle A^2 \rangle$ (see, e.g., Ref. 41).

As shown by Mostovoy and Khomskii, one soliton develops in each chain segment with an odd number of Cu atoms in a strictly one-dimensional system.[22,23] The spatial displacements of the atoms close to the defect are described by

$$A(l) = (-1)^l A_0 \tanh\left(\frac{lc}{\xi}\right), \qquad (1)$$

where c denotes the lattice constant along the chain direction, l is the site index, and ξ is the correlation length (soliton width) which is of the order of $10c$ in the case of CuGeO$_3$.[19,21–23,29,30] In the limit of low soliton density $\langle A^2 \rangle$ decreases linearly with increasing defect concentration (n_S), i.e., $\langle A^2 \rangle / \langle A^2(x=0) \rangle = 1 - 2n_S \xi / c$. If solitons occur only in odd chain segments, i.e., $n_S \simeq 0.5x$, one expects a 10% reduction of $\langle A^2 \rangle$ for 1% Zn doping. Apparently, the experimentally observed decrease of ϵ is much stronger. That means that the number of solitons is larger than that obtained in a strictly one-dimensional treatment, since there is no reason to assume the extremely large soliton width of $\xi = 30c$.

Again following Mostovoy and Khomskii, a larger number of solitons is expected when taking into account an interchain coupling which may originate, e.g., from the coupling of structural deformations in neighboring chains (see also Ref. 30). This interchain coupling ''pins'' the spin defects to the Zn atoms and consequently one obtains $n_S \simeq x$. A similar case has been previously considered by Fukuyama et al.,[21] assuming defects at the doped atom. Again, both descriptions yield a tanh shape of the structural defects at low doping. In order to consider also higher soliton concentrations, the spatial displacements are described in Ref. 21 by

$$A(l, n_S) = (-1)^l A_0 k \, \text{sn}\left(\frac{lc}{k\xi}, k\right), \qquad (2)$$

where sn(x', k) is a Jacobi elliptic function of modulus k, which is determined by the intersoliton distance $d = 1/n_S$.

As shown in Fig. 3, a reasonable agreement between the data and Eq. (2) is obtained for a soliton width of $\xi \simeq 13.6c$, which has been inferred from x-ray-diffraction data for the soliton lattice in the incommensurate high-field phase of pure CuGeO$_3$.[38] This absolute value of ξ revealing the best description of our data crucially depends on the accuracy of the Zn content, whereas the qualitative picture does not. For example, taking the larger nominal Zn concentrations would give a comparable agreement for $\xi \simeq 10c$. Note that we have also added in Fig. 3 two data points measured on Si-doped crystals.[53] Assuming $x_{eff} = 3y$ (see above) these
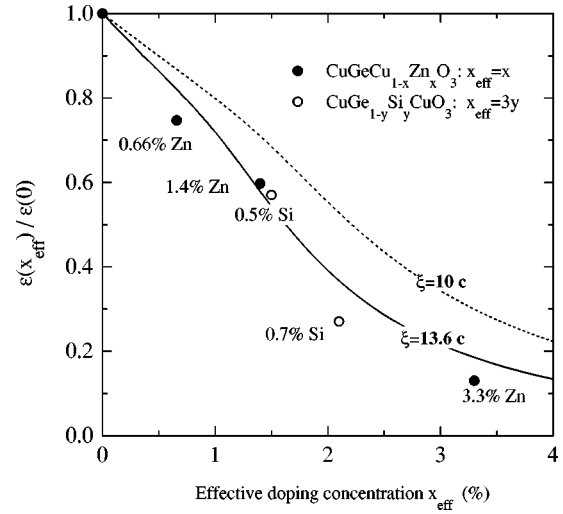

FIG. 3. Normalized low-temperature spontaneous strain as a function of effective doping for Zn and Si-doped CuGeO$_3$. The solid (dashed) line corresponds to a calculation assuming Eq. (2) with a correlation length of $\xi = 13.6$ (10) lattice constants c.

data are also fairly well described, i.e., Zn- and Si-doped crystals with the same T_{SP} and/or T_N exhibit a similar $\langle A^2 \rangle$ at low temperatures.

Figure 3 indicates a good agreement between our experimental findings and a theory assuming defect-induced solitons at each doped Zn atom. We mention, however, that we have assumed a particular spatial shape of the solitons. The spatial modulation of A, as described by Eq. (2), is periodic, i.e., instead of random there are periodic positions of the Zn atoms. However, as long as the overlap of the solitons is not very large, this simplification is not crucial for the result of the average $\langle A^2 \rangle$ considered here. Equation (2) contains a second approximation. The suppression of the order parameter is assumed to be symmetric with respect to the node of the order parameter. If, however, the pinning of the solitons at the defects is important, as suggested by the number of solitons, this symmetry is questionable. The spatial shape of the suppressed dimerization depends on the distance between the soliton and the Zn defect, which is determined by the effective interchain coupling and probably changes with doping due to the decrease of $\langle A^2 \rangle$ (see, also, Ref. 30). Unfortunately, there are—to our knowledge—no corresponding theoretical predictions of the shape of the solitons, which could be compared quantitatively to our data.

In Fig. 4 we plot ϵ at low temperature as a function of T_{SP}, where both axes are normalized to the corresponding values found in pure CuGeO$_3$. Since the doping concentration is not important in this kind of representation, the data measured on Si-doped crystals can be added without any scaling. Indeed, the results for Si- and Zn-doped compounds fall on a common line when plotting ϵ as a function of T_{SP}, as indicated above.

Superimposed to the data there are two lines in Fig. 4. Apparently, a straight line reveals an almost perfect, but purely phenomenological description of the experimental findings. The slope of this line corresponds to $\simeq 2.3$, i.e., $\langle A^2 \rangle$ decreases about 2.3 times stronger upon doping than T_{SP}. Describing the data with this linear dependence leads, however, to a rather strange result. As visible in Fig. 4 the
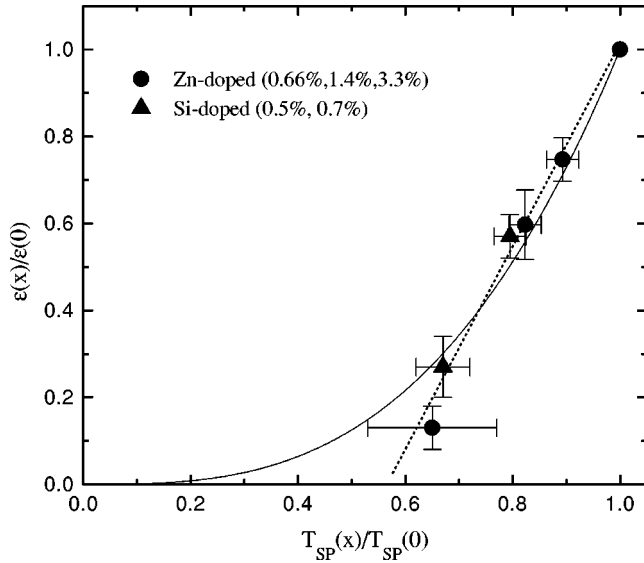
FIG. 4. Normalized low-temperature spontaneous strain in doped $CuGeO_3$ as a function of the normalized SP transition temperature. The dashed line is a guide to the eye and the solid line corresponds to $\epsilon \propto T_{SP}^3$ (see text).

straight line extrapolates to $T_{SP} \approx 0.56 T_{SP}(x=0) \approx 8$ K. The ordering temperature seems to remain high, while the average order parameter at zero temperature vanishes. Remarkably, this strange description is reminiscent of various experimental studies of the (x,T) phase diagrams of doped $CuGeO_3$.[64,4,6,10,14,11,12] In none of these studies has a spin-Peierls transition with a T_{SP} below about 8 K been found.

We stress, however, that the straight line in Fig. 4 does not imply a linear decrease of T_{SP} from 14.3 down to 8 K with increasing x. As visible in Fig. 3, a linear decrease of ϵ is only present for small doping. For larger concentrations the decrease of ϵ strongly reduces as expected from the soliton picture, since the solitons start to overlap. Therefore, assuming a linear dependence between T_{SP} and ϵ as suggested by the straight line in Fig. 4 and calculating $\epsilon(x)$ from Eq. (2), yields a linear decrease of T_{SP} only for low doping ($x \lesssim 2\%$). For larger x, however, T_{SP} saturates and approaches very slowly the minimum $T_{SP} \approx 8$ K with increasing x.

At first glance, this seems to be in striking discrepancy with the (x,T) phase diagrams reported from susceptibility measurements, which only show a linear decrease of T_{SP}.[4,6,14,5,10] However, in the magnetic susceptibility the signatures of the SP transition disappear already at rather low doping.[4,6,14,5,10] For example, a recent susceptibility study of $Cu_{1-x}Zn_xGeO_3$, which was performed on identically prepared and characterized single crystals, reveals no SPT for $x=3.3\%$.[14] For the same concentration our data show a broad crossover phenomenon to a SP-like state which occurs, however, at a rather large temperature of about 9.5 K. Note that this value is much larger than that obtained from an extrapolation of the linear decrease at small x, revealing $T_{SP} \lesssim 7.5$ K.

Remarkably, the phase boundary which is obtained, if we assume Eq. (2) and the straight line in Fig. 4, has also been reported in the literature. It is essentially identical to that extracted from neutron diffraction on $Cu_{1-x}Zn_xGeO_3$ in

Refs. 11,12. However, in our opinion, the corresponding phase boundary between the U and the low-temperature phase, which is present up to high Zn contents, should not be interpreted as a $T_{SP}(x)$. From our raw data in Fig. 1 it is apparent that the shape of anomalies changes drastically upon doping. Whereas α shows rather well defined SPT's for small x, the data for the sample with $x=3.3\%$ signal a broad crossover to a ''SP''-like state. It is the characteristic temperature of the crossover phenomenon, which remains high and replaces the T_{SP} of a SPT in a thermodynamic sense. The latter clearly does not exist anymore for $x=3.3\%$. Such a change from a SPT to a gradual crossover into a SP-like state has also been anticipated from recent ultrasound measurements.[58] Moreover, this description is supported by a recent neutron-diffraction study, which confirms the appearance of weak superstructure reflections at high doping levels.[67] However, according to this study these small and broad peaks have to be attributed to short-range order phenomena.

Taking into account that the meaning of the T_{SP} given in Fig. 4 changes at high doping, and therefore considering only the concentration range with rather well-defined SPT, offers an alternative interpretation of the data. As shown by the solid line, the data for $x<3.3\%$ are also well described by the power law $\langle A^2 \rangle \propto T_{SP}^3$. We emphasize that this cubic dependence is not purely phenomenological. It is related to the theoretical results for a SPT with homogeneous dimerization. Both the theory of Cross and Fisher[34] as well as numerical calculations for frustrated chains[68] yield that the ($T=0$) dimerization A of the magnetic exchange scales with the spin gap Δ at zero temperature via $|A|^{2/3} \propto \Delta$. Moreover, it is reasonable to assume that T_{SP} is proportional to $\Delta(0)$, since the experimentally observed gap ratios $2\Delta(0)/k_B T_{SP}$ are close to the BCS value of 3.52 for SP compounds. Taking into account these results leads to the following scaling between T_{SP} and ϵ at zero temperature:

$$\epsilon(T=0) \propto A^2(T=0) \propto \Delta^3(T=0) \propto T_{SP}^3. \qquad (3)$$

This scaling corresponds to our findings in doped $CuGeO_3$ for small x, if we replace A^2 by its spatial average $\langle A^2 \rangle$. Thus, our data suggest that the scaling between the average dimerization and T_{SP} does not significantly differ from that in a homogeneous SP compound as long as a well-defined SPT is present.[69] Knowing the scaling between the low-temperature $\langle A^2 \rangle$ and T_{SP}, we can quantitatively derive the reduction of T_{SP} as a function of x in a very simple way. Once the correlation length ξ is known, the microscopic soliton picture predicts $\epsilon(x,T \to 0)$ (see Fig. 3). T_{SP} is then obtained from the scaling $T_{SP} \propto [\epsilon(T \to 0)]^{1/3}$ as well. Thus, a theoretical explanation of the scaling between $\langle A^2 \rangle$ and T_{SP}, i.e.. the justification of our extension of the Cross-Fisher result to doped systems, simultaneously reveals a quantitative theoretical explanation of $T_{SP}(x)$ in Zn-doped $CuGeO_3$.

IV. THERMODYNAMIC PROPERTIES OF $Cu_{0.986}Zn_{0.014}GeO_3$ IN EXTERNAL FIELDS

A. Thermal expansion of $Cu_{0.986}Zn_{0.014}GeO_3$

Figure 5 shows the thermal-expansion coefficient α_a of the sample with a Zn content $x=1.4\%$ measured in external
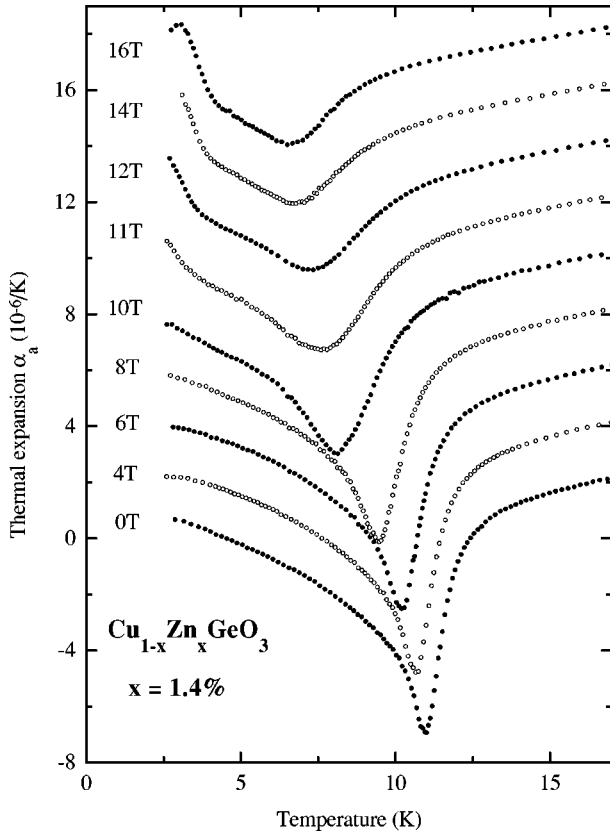
FIG. 5. Thermal-expansion coefficient along the a axis of $Cu_{0.986}Zn_{0.014}GeO_3$ for different magnetic fields given in the figure. Curves are shifted by $2 \times 10^{-6}/K$ for clarity.

fields between 0 and 16 T. For $H < 10$ T the transition temperature decreases with increasing field, whereas the size of the anomaly does not change strongly. Qualitatively, these findings at low fields compare well with those reported for pure $CuGeO_3$.[43] Pronounced differences are, however, present at higher fields. In the Zn-doped compound the anomaly at the SP transition drastically broadens for fields above 10 T. Following the above discussion of the doping dependence, these data on the Zn-doped compound reveal some evidence for a change from a rather well-defined SPT in zero field to a short-range order phenomenon in high magnetic fields. In particular, this pronounced additional broadening of the transition occurring in high fields, is obviously not a consequence of sample inhomogeneities, but represents an ''intrinsic'' property of doped $CuGeO_3$.

Besides this broadening, a further surprising finding is apparent from Fig. 5. In high fields, a second rather sharp anomaly occurs at low temperatures signaling the development of long-range AFM order. Note the similarity to the zero-field data at higher doping. Unfortunately, our measurements are restricted to temperatures above about 2.5 K and we cannot follow the field dependence of T_N at lower fields. A pronounced increase of T_N in high magnetic field is, however, apparent from our data. It is worthwhile mentioning that the magnetic field is applied along the a axis in our experiments. Thus, the unusual field dependence of T_N is not related to the spin-flop transition which only occurs for fields parallel to c (Refs. 4,58,56,6) (see below).
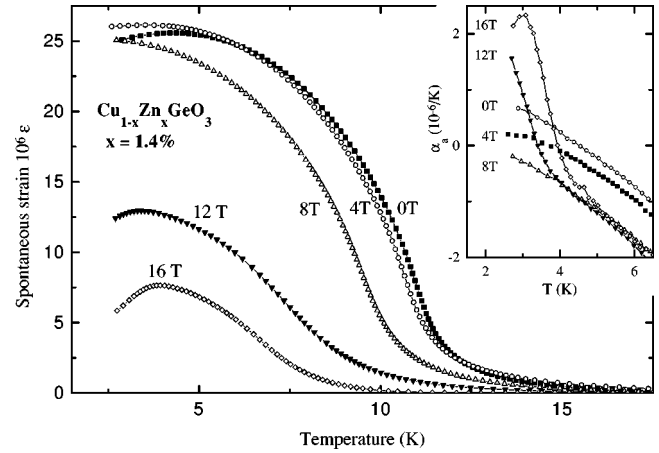

FIG. 6. Spontaneous strains of the lattice constant a for different magnetic fields given in the figure. Inset: Thermal-expansion coefficient at low temperatures for some representative magnetic fields.

Investigating the low-field and low-temperature data in more detail reveals precursors of the low-temperature anomaly due to AFM order also in zero field. This can be extracted from Fig. 6, where the spontaneous strains derived from the data in Fig. 5 are displayed for some representative magnetic fields. For $H = 0, \epsilon$ decreases slightly with decreasing temperature below about 4 K or, equivalently, the thermal-expansion coefficient increases with decreasing temperature below 4 K as shown in the inset of Fig. 6. Both observations strongly suggest the proximity of a further ordering phenomenon, since α has to approach 0 at $T = 0$ for general thermodynamic reasons. Moreover, the behavior at $H = 0$ is qualitatively very similar to the findings in high fields where the second phase transition is apparent. In contrast to the data in zero and high fields, no anomalous low-temperature behavior is present in the thermal expansion and/or the spontaneous strain at intermediate fields 4 T $< H \lesssim 10$ T. Thus, the data suggest a nonmonotonous field dependence of the AFM instability. Whereas small magnetic fields suppress long-range magnetic order, a strong increase of T_N is found, if the field exceeds ~ 10 T.

Neglecting the additional anomaly due to AFM order, the field dependence of ϵ found in the Zn-doped compound compares well to that in pure $CuGeO_3$.[43] For fields smaller than $H \simeq 10$ T, the spontaneous strain extrapolates to a nearly field-independent zero-temperature value. Further increasing the magnetic field leads to a drastic decrease of ϵ in a rather narrow field range followed by a weaker decrease for fields above about 12 T. This field dependence of ϵ is related to the field-driven transition from the dimerized to the incommensurate phase, which will be discussed in detail below in the context of the magnetostriction data.

B. Specific heat of $Cu_{0.986}Zn_{0.014}GeO_3$

In Fig. 7 the specific heat of the Zn-doped crystal with $x = 1.4\%$ is shown. The strong suppression of the specific-heat anomaly at the SPT with increasing field is apparent. Anomalies due to AFM order are not found in the entire temperature and field range. At first glance this is very surprising, since the thermal expansion in high magnetic fields, which was measured on the same crystal, shows clear
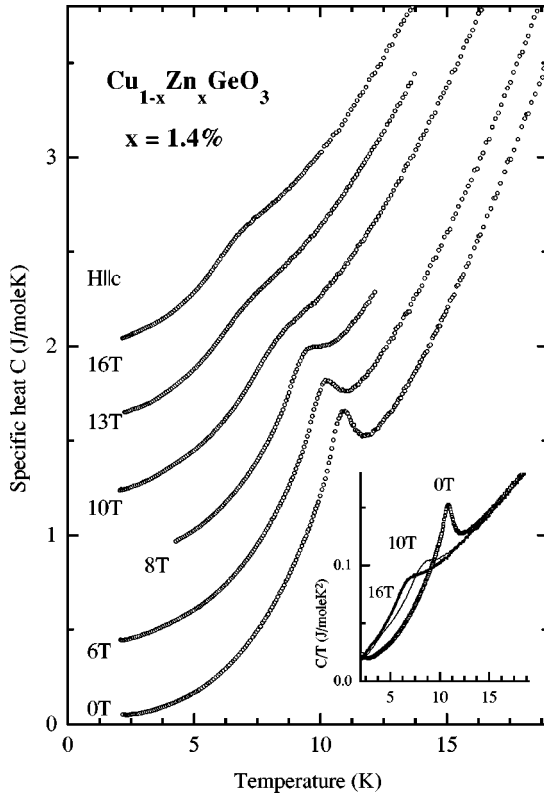
FIG. 7. Specific heat of $Cu_{0.986}Zn_{0.014}GeO_3$ measured in different magnetic fields ($H \| c$) given in the figure. Curves are shifted by 0.4 J/mole K for clarity. Inset: C/T vs T for three representative magnetic fields.

anomalies. One reason is the different orientation of the magnetic field which was applied parallel to the c axis in the specific-heat measurements, leading to a slightly smaller T_N (see below). In addition we have, however, to conclude that the anomalies of the specific heat due to AFM in high magnetic fields are much smaller than those of α. Therefore no precursors of the corresponding anomaly are observable which are clearly present in α for the same field orientation and temperature range (see Fig. 13 below). Note, that a similar conclusion can also be drawn from the data recently reported for a Si-doped $CuGeO_3$ crystal with a slightly higher T_N.[45,46]

The suppression of the specific-heat anomaly at the SPT as a function of H is very large. The size of the anomaly reduces already for $H \lesssim 8$ T and, even for this moderate fields, there is a pronounced broadening of the transition. The width of the anomaly further increases continuously with increasing H. For $H \gtrsim 10$ T it is not possible to extract a well-defined T_{SP} from the specific-heat data. An anomaly due to a broadened SPT is, however, visible when plotting C/T vs T as shown in the inset of Fig. 7. Comparison of the anomalies of the thermal expansion and the specific heat, reveals no qualitative differences in the high-field range. Both quantities indicate a crossover behavior instead of a well-defined SPT which is signaled at $H=0$. However, a quite different field dependence of both, size and shape of the anomalies is found at intermediate fields. Whereas α signals a sharp transition for $H=8$ T, the specific-heat anomaly measured on the same sample is already strongly reduced and broadened compared to that for $H=0$.[70] It is
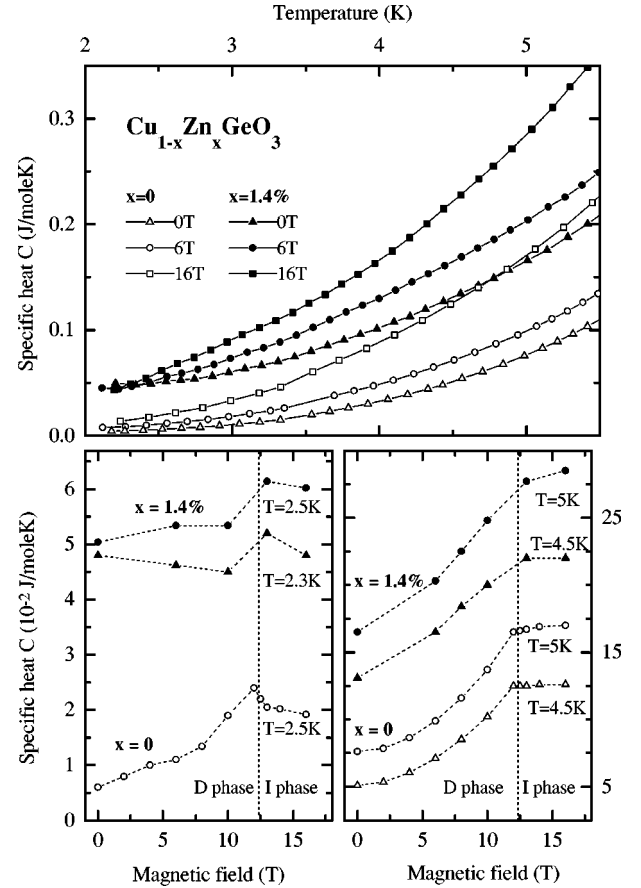

FIG. 8. Upper panel: Temperature dependence of the low-temperature specific heat of pure $CuGeO_3$ (open symbols) and $Cu_{0.986}Zn_{0.014}GeO_3$ (closed symbols) for three magnetic fields given in the figure. Lower panel: Magnetic-field dependence of the specific heat of pure $CuGeO_3$ (open symbols) and $Cu_{0.986}Zn_{0.014}GeO_3$ (closed symbols) for different temperatures given in the figure.

worthwhile mentioning that a similar difference is observed in the concentration dependence of the anomalies in zero field.[53]

A possible origin of these different field dependences are the different degrees of freedom which are relevant for the thermal expansion and specific-heat anomalies. $\Delta \alpha$ is determined mainly by the structural order parameter, i.e., the lattice dimerization, whose zero temperature value hardly changes for fields below the D/I transition, since it is mainly a property of the nonmagnetic ground state. The specific-heat anomaly is closely related to the decrease of the magnetic entropy related to the spin gap. In contrast to the lattice dimerization, the spin gap Δ markedly decreases with increasing H due to the Zeeman splitting of the triplet states.

The relevance of different degrees of freedom for α on the one and C on the other hand is also seen from the low-temperature behavior. There is a drastic change of C upon doping, indicating a drastic doping dependence of the low energy excitation spectrum in the D phase. This is apparent when comparing the specific heat of pure and doped $CuGeO_3$. As shown in Fig. 8, the specific heat for $x=1.4\%$ is about one order of magnitude larger than that of $CuGeO_3$ at the lowest temperature of our measurements (~ 2.3 K). It is well known that C for $x=0$ (and $H=0$) is well described by the sum of a usual phonon contribution βT^3

($\beta \simeq 0.3$ mJ/mole K^4) and an activated behavior [$\exp(-\Delta/T)$], representing the magnetic singlet triplet excitations (see, e.g.. Ref. 50). A similar description is impossible for the Zn-doped compounds (see, also, Ref. 53). Since the Debye-like phonon contribution does not change significantly for such small Zn concentrations, a drastic increase of the magnetic excitations in the dimerized phase is inferred from the much larger low-temperature specific heat (see, also, Ref. 71). A possible origin of these additional excitations is obvious from the soliton picture mentioned above. Close to the doping-induced defects, ''loose'' spins and AFM correlations develop which are responsible for the Néel ordering occurring at low temperatures. It is straightforward to attribute the additional specific heat C_{dop} to these degrees of freedom. Note that these additional low-energy excitations, which cause an additional specific heat upon doping, are also found in several theoretical studies of disordered SP systems.[24,25]

In order to extract the temperature dependence of C_{dop} one has to separate it from the usual spin excitations in the spin-Peierls phase. Besides the additional doping-induced excitations, there are singlet triplet excitations related to the (pseudo) gap in the excitation spectrum. In order to illustrate the significance of these two contributions we compare the magnetic-field dependences of C for $x=0$ and $x=1.4\%$ in the lower part of Fig. 8. At low temperatures C hardly changes with H in the doped compound, whereas a pronounced increase is present in the dimerized phase of pure CuGeO$_3$. The latter obviously arises from the decrease of the singlet triplet gap.

The absence of a corresponding increase for $x=1.4\%$ confirms that the low-temperature specific heat is dominated by excitations which differ from the singlet triplet excitations. Moreover, the field independence of the total C implies that there are two compensating field dependences, i.e., C_{dop} decreases with increasing field. The importance of this field dependence for the total specific heat vanishes at higher temperatures. At $T=4.5$ K, C for $x=0$ and $x=1.4\%$ exhibit the same qualitative behavior as a function of H. Both increase strongly as expected from the decrease of the singlet triplet (pseudo) gap. In the doped compound this increase of C is even larger by a factor of about 1.5 due to a smaller $H=0$ (pseudo) gap which has to be compared to the H-dependent Zeeman energy.

Similarities of the specific heat for $x=0$ and $x=1.4\%$ are also observed when comparing the temperature dependences. Though the absolute value of C is much larger in the doped compound, the temperature derivatives of C are similar for $x=0$ and $x=1.4\%$, indicating that C_{dop} does not change strongly as a function of T (see the data for $H=0$ in Fig. 8). This can be used to separate the different contributions to C. Indeed, investigating the temperature derivatives of C, it is possible to resolve clear consequences of the singlet triplet (pseudo) gap for $x=1.4\%$. A corresponding analysis is shown in the left part of Fig. 9. In order to obtain the magnetic contribution C_{mag}, we have subtracted the phonon contribution $\beta T^3 (\beta=0.3$ mJ/mole K^4) determined for pure CuGeO$_3$. Assuming a sum of two contributions to C_{mag} of the form
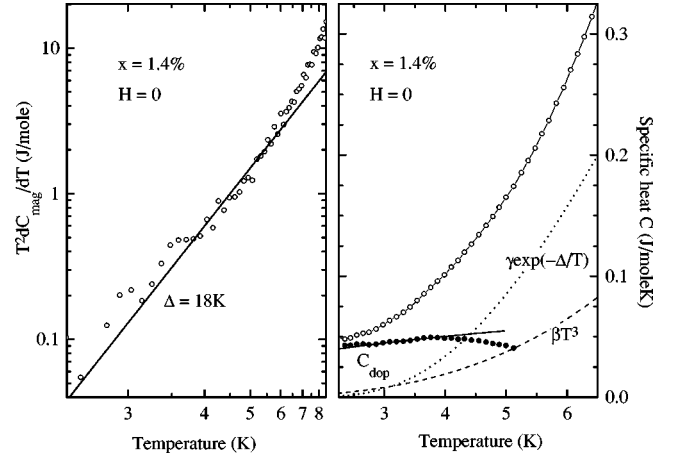
$$C_{mag} = \gamma e^{-\Delta/T} + C_{dop}, \tag{4}$$

FIG. 9. Left: Arrhenius plot of $T^2 \partial C / \partial T$ in Cu$_{0.986}$Zn$_{0.014}$GeO$_3$ (see text). The straight line corresponds to an activated behavior with a gap of $\Delta = 18$ K. Right: Separation of the low-temperature specific heat of Cu$_{0.986}$Zn$_{0.014}$GeO$_3$($\bigcirc$) into a sum of phonon (βT^3, dashed line), singlet triplet (activation law, dotted line) and a doping induced contributions ($\bullet$) (see text). The solid line corresponds to $C \propto T^{0.4}$ (see text).

where Δ denotes the singlet triplet (pseudo) gap and γ is a constant, implies for the temperature derivative

$$\frac{\partial C_{mag}}{\partial T} = \gamma \frac{\Delta}{T^2} e^{-\Delta/T} + \frac{\partial C_{dop}}{\partial T}. \tag{5}$$

As displayed in Fig. 9, the quantity $T^2 \partial C_{mag} / \partial T$ follows a straight line in an Arrhenius plot for temperatures below about 6 K. This is the behavior expected from Eq. (5), if C_{dop} (and Δ) does not change strongly with T. A gap of $\Delta \simeq 18$ K is obtained from the slope in the Arrhenius plot. Thus, according to this analysis, the reduction of the gap upon doping $\Delta(x=1.4\%)/\Delta(x=0) \simeq 0.8$ agrees well with the reduction of T_{SP}. Moreover, the temperature range $T \lesssim T_{SP/2}$, showing the simple activated behavior for $x=1.4\%$, compares well to that found in pure CuGeO$_3$.[50] Note that at higher temperatures the decrease of Δ causes an enhanced specific heat. From the linear fit in the left part of Fig. 9 it is also possible to extract $\gamma \simeq 2$ J/mole K which is reduced compared to the value found in the pure compound (3.6 J/mole K).

Since we have now a reasonable description of the specific heat due to the singlet triplet excitations which was obtained without any assumption for C_{dop}, it is possible to separate the different contributions to the specific heat in the Zn-doped crystal. The result is shown in the right part of Fig. 9. At low temperatures $C_{dop} \sim 0.05$ J/mole K is by far the largest contribution, whereas the temperature dependence of C is determined in the entire temperature range by the two other contributions. Unfortunately, the above analysis is impossible for C in high fields, since corresponding data on CuGeO$_3$ show, that there are strong deviations from a simple activated behavior for the singlet triplet excitations. However, from our interpretation of the $H=0$ data and the observed field independence of the total C, it is apparent that external fields strongly suppress C_{dop}, since the singlet triplet gap decreases. Comparing the field dependence of C mea-

sured for $x=1.4\%$ and $x=0$ and taking into account the smaller $\Delta(H=0)$ for the doped compound, one estimates a decrease of C_{dop} at $T \sim 2.5$ K of about 30% to 50% in a field of 10 T.

Considering a disordered quasi-one-dimensional antiferromagnet gives a possible interpretation of these findings. On the one hand, it has been argued recently[24,25] that solitonlike domain walls in a SP system and Heisenberg chains with random exchange constants yield a similar low-energy density of states which determines the thermodynamic properties at low temperatures. On the other hand, it is well known that random magnetic exchange parameters cause unusual temperature and field dependences of the magnetization and the specific heat[72] (see also the application to disordered SP systems in Refs. 24,25,16). In particular, in the low-field and low-temperature range, the magnetic susceptibility is described by a power law $\chi \propto T^{-\nu}$ with an exponent $\nu < 1$. This temperature dependence interpolates between that of one dimensional chains with homogeneous J, leading to $\chi \rightarrow$ const, and the behavior of noninteracting spins with a Curie susceptibility ($\nu = 1$). In a system with a random J and a distribution function $W(J) \rightarrow 0$ for $J \rightarrow 0$ the divergence of χ still exists, but the increase is smaller than in the case of free spins, leading to the above-mentioned power law with $\nu < 1$.

The exponent ν measuring the disorder determines also the field and temperature dependences of C. Bulaevskii *et al.* find[72]

$$C(T,H=0) \propto T^{1-\nu} \quad \text{for } T \rightarrow 0,$$

$$C(T,H) \propto T\left(\frac{g\mu_B H}{k_B}\right)^{-\nu} \quad \text{for } \frac{g\mu_B H}{k_B T} \gg 1. \quad (6)$$

Taking a disorder parameter $\nu \simeq 0.6$, these results reproduce the strong field dependence of C_{dop} estimated from our data. Moreover, the weak temperature dependence of C_{dop} above 2 K is also consistent with this value of ν as indicated in Fig. 9. We mention that our measurements of the magnetic susceptibility confirm this description (see also Ref. 16). However, an unambiguous determination of ν is impossible, since there are again several contributions. Nevertheless, the calculations for a disordered quasi-one-dimensional antiferromagnet reveal a reasonable explanation of the strange T and H dependences of C_{dop} in the D phase in agreement with the theoretical predictions.[24,25] However, we emphasize that our data neither allow us to determine unambiguously the corresponding temperature dependences nor to extract precise values of the disorder parameter ν. On the one hand, the available temperature range ($T_N < T \lesssim T_{SP}/2$) is too small. On the other hand, it is difficult to separate the different contributions present in both, C and χ.

Finally, we shortly comment on a further difference between the field dependences of the specific heat for $x=0$ and $x=1.4\%$, respectively. At the transition field ($H_{D/I}$) to the incommensurate phase, the low-temperature specific heat decreases in pure CuGeO$_3$, whereas it increases in the doped compound (see Fig. 8). In the D phase there is a large C_{mag} due to the singlet triplet excitations, since Δ is strongly reduced for $H \simeq H_{D/I}$. The character of the low-lying excitations changes when entering the I phase in pure CuGeO$_3$.

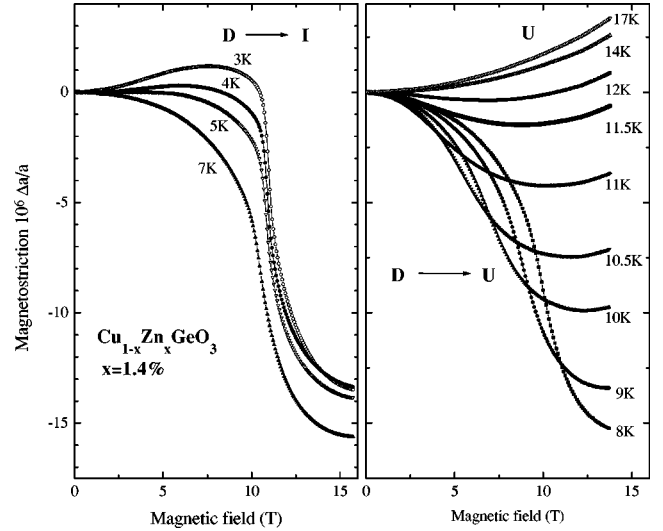FIG. 10. Magnetostriction of the lattice constant a in Cu$_{0.986}$Zn$_{0.014}$GeO$_3$ measured at different temperatures given in the figure.

Here, C_{mag} follows a simple T^3 law[50] due to a new gapless "phason" mode, which appears as a consequence of the *regular* periodic incommensurate modulation of the dimerization.[73] Related to this change of the excitations, C_{mag} as well as the magnetic entropy measuring the "magnetic disorder" decrease at $H_{D/I}$ in pure CuGeO$_3$ for 2 K $\lesssim T \lesssim 8$ K. In contrast, this "magnetic disorder" increases at $H_{D/I}$ in the Zn-doped crystal.

C. Magnetostriction of Cu$_{0.986}$Zn$_{0.014}$GeO$_3$: The D/I phase transition

The two properties investigated so far, i.e., the thermal expansion and the specific heat, do not allow for a detailed study of the field-induced transition from the dimerized to the incommensurate phase. This is possible by measuring the magnetostriction, i.e., the field dependence of the lattice constant at a fixed temperature. In Fig. 10 the results of these measurements along the a axis ($\Delta a/a$) of the Zn-doped crystal with $x=1.4\%$ are displayed. Below about 8 K a sharp decrease of the lattice constant occurs, signaling a first-order phase transition at a field $H_{D/I} \simeq 11$ T, which does not change strongly as a function of temperature. At higher temperatures this jumplike decrease disappears and instead anomalies due to the continuous phase transition between the dimerized and the uniform phase are present for temperatures $T \lesssim T_{SP}(0) \simeq 11.5$ K. In this temperature range both, the transition fields as well as the total magnetostriction strongly decrease with increasing T. For temperatures above $T_{SP}(0)$ there are no phase transitions. The lattice constant now increases with increasing H due to the magnetoelastic coupling in the uniform phase.[55,44,43]

The magnetostriction of the Zn-doped compound shows many similarities with that of pure CuGeO$_3$, which is discussed in detail in Ref. 44. The size of the anomalies is reduced due to the smaller spontaneous strain, which is closely related to the magnetostriction[43,41] below $T_{SP}(H = 0)$. This relationship reads
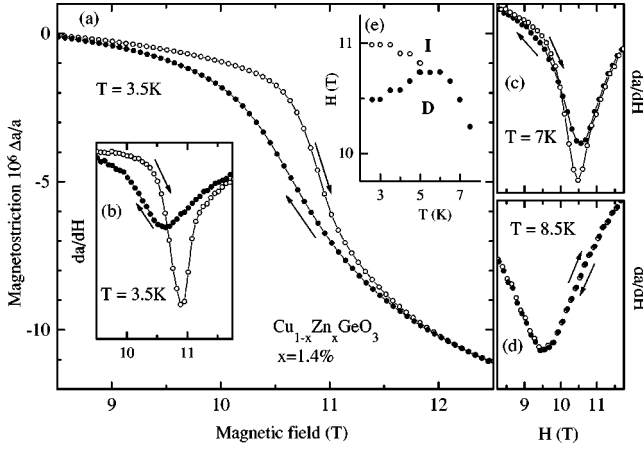
FIG. 11. (a) Magnetostriction of $Cu_{0.986}Zn_{0.014}GeO_3$ measured along the a direction at $T = 3.5$ K with increasing ($\bigcirc$) and decreasing ($\bullet$) field. (b)–(d) Field derivatives of the lattice constant a measured with increasing ($\bigcirc$) and decreasing ($\bullet$) fields at different temperatures given in the figure. (e) Transition fields as determined from the peaks of the field derivatives of the lattice constant a measured with increasing ($\bigcirc$) and decreasing ($\bullet$) fields.

$$\epsilon(H,T) = \frac{\Delta a}{a}(T,H) - \frac{\Delta a}{a}(T_0,H), \qquad (7)$$

where T_0 denotes a temperature larger than $T_{SP}(H=0)$. Thus, the additional magnetostriction in the spin-Peierls phase measures $\epsilon(H)$.[43] The differences of the spontaneous strains in Zn-doped and pure $CuGeO_3$ imply also a different magnetostriction. At low temperatures, e.g., at $T = 3$ K, a pronounced increase of the lattice constant is observed in the dimerized phase with increasing H. This magnetostriction is a consequence of the suppression of the Néel order which we have inferred above from the field dependence of α and ϵ (see Fig. 6). Similarly, the decrease of the lattice constant due to the AFM order in the I phase leads to an additional contribution to the magnetostriction at the D/I transition at very low temperatures. We mention that other findings from the thermal-expansion data, as, e.g., the broadening of the U/I transitions, are also confirmed by the magnetostriction measurements, when analyzing the data according to Eq. (7).

We turn now to the field-driven D/I transition which cannot be studied in detail measuring the thermal expansion. As has been pointed out in several theoretical treatments, impurities are important for the discussion of this phase transition. It is, for example, argued that the pinning of solitons due to defects might be the origin of the first-order nature of the D/I transition usually observed.[74,2] The first-order transition leads to an hysteresis of the magnetostriction and, therefore, the data in Fig. 10 which were measured with increasing field slightly differ from those obtained with decreasing field as displayed in Fig. 11. With increasing field the transition is observed at higher fields on the one hand. On the other hand, the change of the lattice constant occurs in a much smaller field range, i.e., the D/I transition upon increasing H is much sharper than the I/D transition upon decreasing H. Both observations are qualitatively explained, if we assume a pinning potential for the field induced structural modulation in the I phase. We emphasize that these hysteresis loops mark-

edly differ from those observed in pure $CuGeO_3$, where the widths of the D/I and I/D transitions do not differ significantly.[44]

Further differences between pure and doped $CuGeO_3$ are revealed, when comparing the sizes of the field hysteresis and their temperature dependences. From the peaks of the field derivatives of the lattice constant (see Fig. 11) we have extracted the transition fields $H_{D/I}$ for increasing and decreasing H, respectively. At low temperature an hysteresis $\Delta H_{D/I}$ of about 0.5 T is obtained which is more than a factor of two larger than in pure $CuGeO_3$. With increasing temperature, $\Delta H_{D/I}$ decreases strongly and for $T \gtrsim 6$ K the peaks in the field derivatives of the lattice constant reveal $\Delta H_{D/I} \simeq 0$. There is, however, still a small hysteresis of the magnetostriction close to the phase transition. As shown in Fig. 11(c) the transition at $T = 7$ K upon decreasing field is still slightly broader, whereas at higher temperatures, e.g., at $T = 8.5$ K [Fig. 11(d)], no hysteresis is resolved.

The D/I phase boundary, as extracted from the magnetostriction, is also shown in an inset of Fig. 11. Both the temperature dependence of $H_{D/I}$ as well as that of the hysteresis which we observe in the Zn-doped crystal markedly differ from the corresponding observations in pure $CuGeO_3$ as will be discussed in the next section.

V. MAGNETIC FIELD TEMPERATURE PHASE DIAGRAMS OF $Cu_{1-x}Zn_xGeO_3$

In the preceding section we have only considered data measured for the crystal with a Zn doping of $x = 1.4\%$. Thermal expansion as a function of H as well as magnetostriction have also been measured for the two other compositions $x = 0.66\%$ and $x = 3.3\%$. For the smaller Zn content we do not find any signatures of the AFM order in the temperature range of our study ($T \gtrsim 4$ K in this case). The findings at the SPT compare well with those reported above for $x = 1.4\%$. In Fig. 12 the corresponding phase diagram extracted from thermal expansion and magnetostriction data is shown. It is similar to that reported by Fronzes et al. for a crystal with a slightly smaller x.[58] In the upper part of the figure we show our findings along the a axis for $H||a$. Taking into account the slightly different g values measured by ESR,[75–77] the same phase diagrams are obtained along the two other lattice directions and field orientations, as shown in the lower part of Fig. 12. Note that not only the phase boundaries, but also the field hysteresis of the D/I transition is the same for the three lattice and field directions, when plotting the data in reduced scales.

The differences between the findings at the SPT's for $x = 1.4\%$ and $x = 0$, which we have extracted from the data in the last section, are less pronounced but still present, when comparing the data for $x = 0.66\%$ and $x = 0$. The U/I transitions at high fields are again significantly broader than the U/D transitions at low fields (see below). Moreover, the findings at the field-driven D/I transition for $x = 0.66\%$ smoothly interpolate between those for $x = 0$ and $x = 1.4\%$. At low temperatures the field hysteresis for $H||a$ amounts to 0.35 T, whereas 0.15 and 0.5 T are observed for $x = 0$ (Ref. 44) and $x = 1.4\%$, respectively. A similar systematic trend as a function of doping is found, when comparing the temperature dependence of $\Delta H_{D/I}$. For $x = 0.66\%$ we find $\Delta H_{D/I} \simeq 0$ at
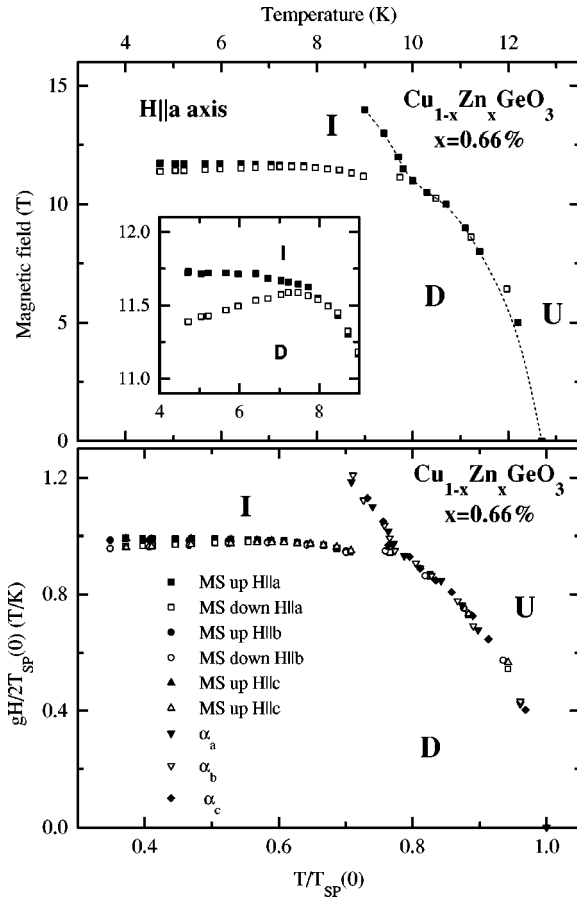
FIG. 12. Magnetic-field temperature phase diagram of $Cu_{0.9934}Zn_{0.0066}GeO_3$ as determined from thermal expansion and magnetostriction (MS). Upper panel: $H\|a$. Inset: D/I phase boundary on an extended scale as determined upon increasing (——) and decreasing ($\square$) fields . Lower panel: Phase diagram obtained along the three lattice directions and field orientations plotted in reduced scales. The g values are taken from ESR measurements (Refs. 75–77).

FIG. 13. Upper panel: Thermal expansion of $Cu_{0.986}Zn_{0.014}GeO_3$ along the b (left) and the c direction for three representative fields. Lower panel: (H,T) phase diagram of $Cu_{0.986}Zn_{0.014}GeO_3$ as derived from the thermal expansion and the magnetostriction of the b axis for $H\|b$. T_N is smaller than the lowest temperature accessible in our experiment for fields below 10 T. The dotted line shown in this field range represents an upper boundary for T_N.

temperatures above 8 K. For the higher Zn content, the two boundaries merge already at $T \lesssim 6$ K, whereas in pure $CuGeO_3$ the magnetostriction reveals a finite $\Delta H_{D/I}$ up to the Lifshitz point at $T \simeq 11$ K.[44] Thus, the hysteresis of the D/I transition systematically changes with increasing Zn doping. It is worthwhile mentioning that the differences noted for the D/I phase boundary, which systematically develop as a function of x in $Cu_{1-x}Zn_xGeO_3$, are also found when comparing the findings in pure $CuGeO_3$ with those in the organic SP systems $MEM(TNQ)_2$ (Ref. 78) and TTF-CuBDT.[79] In the latter the $\Delta H_{D/I}$ are much larger at low temperatures ($\simeq 0.1 H_{D/I}$) and disappear for temperatures well below the Lifshitz point. In contrast the hysteresis at the D/I transition observed in a third organic SP compound, TTF-AuBDT, is very small.[42] In Ref. 80 it was suggested to attribute these differences observed for the different organic SP compounds to a pinning of solitons at defects. This interpretation is strongly supported by our findings on Zn-doped $CuGeO_3$ which clearly show a systematic increase of the hysteresis at low temperature with increasing number of defects.

We turn now to the phase diagram of the crystal with a Zn doping of $x = 1.4\%$ which is shown in Fig. 13. In the preced-
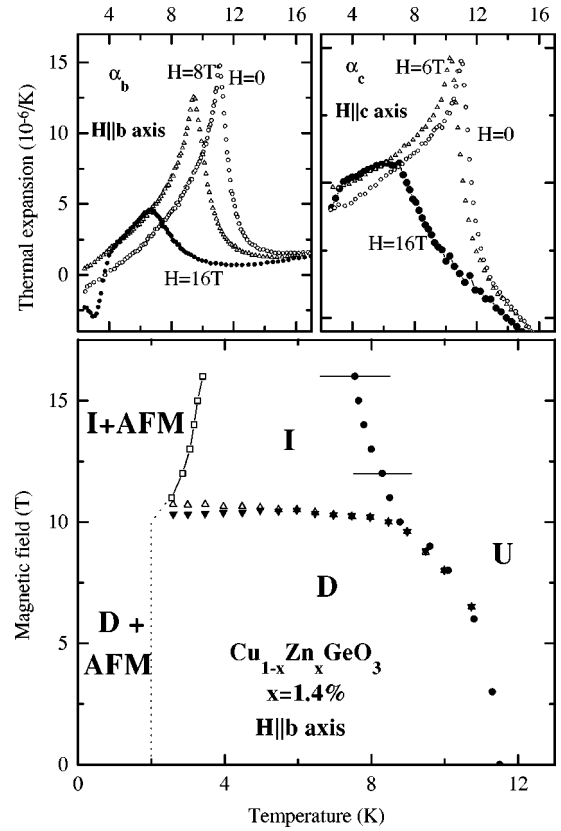
ing sections we have shown the data obtained along the a direction of the crystal for $H\|a$. The findings along the two other directions are very similar, when taking into account the different g values. For the phase boundaries related to the SPT there is no resolvable difference as in the case of $x = 0.66\%$. Moreover, other observations described for the lattice constant a in the preceeding sections are also found for the other lattice and field orientations.

The pronounced additional broadening of the U/I transition does occur for all three lattice directions, as shown by the representative data in the upper part of Fig. 13. Moreover, for $H=0$ the low-temperature thermal expansion of all lattice constants indicates a further phase transition below $\simeq 2$ K, i.e., the α_i do not approach 0. This additional contribution is suppressed in moderate fields. The behavior we find for the AFM order observable at high fields is also qualitatively the same for all three lattice directions. However, for $H\|c$ our data show only the high-temperature part of the corresponding anomaly at $H=16$ T (see upper part of Fig. 13), signaling a slightly smaller T_N than for the two other field orientations. This smaller T_N is most likely related to the spin-flop transition which is known to occur in the AFM phase for this field orientation, since the c axis is the easy axis of the magnetization.[4,58,56,6] In the case of the $x = 1.4\%$ sample we cannot directly see this transition due to the limited temperature range of our experiment. For samples
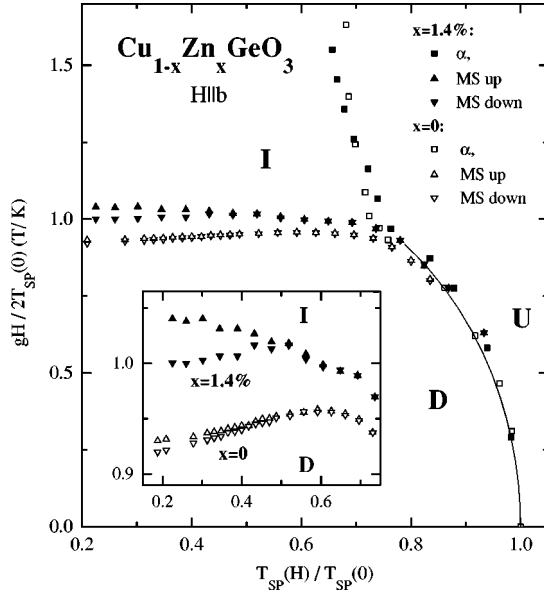
FIG. 14. Comparison of the (H,T) phase diagrams of $Cu_{0.986}Zn_{0.014}GeO_3$ (full symbols) and $CuGeO_3$ (open symbols) in reduced scales. The solid line is based on the theoretical prediction of Cross (Refs. 35,81). Inset: Comparison of the D/I phase boundaries in $Cu_{0.986}Zn_{0.014}GeO_3$ (closed symbols) and $CuGeO_3$ (open symbols) in reduced scales.

with larger T_N, we find this spin-flop transition at fields below $\simeq 1.5$ T applied parallel to the c axis in agreement with several other studies of doped $CuGeO_3$.[4,58,56,6] Neglecting this small field anisotropy of the AFM ordered state, which is apparently related to small corrections to the isotropic Heisenberg exchange, we observe the same behavior for all three lattice directions. Antiferromagnetism is strongly enhanced in an external field which is large enough to induce the incommensurate modulation. Moreover, note the opposite signs of the anomalies at T_N and T_{SP} present for all lattice directions. Both observations indicate a relationship between the dimerization and the AFM order which we will discuss in detail below.

Concerning the SPT, the phase diagrams for the Zn-doped compounds ($x=0.66\%$ and $x=1.4\%$) show the expected features in agreement with several previous studies of the field temperature phase diagrams of doped $CuGeO_3$.[59,56,45,46,58] In Fig. 14 we compare quantitatively the phase diagrams for $x=0$ and $x=1.4\%$. Normalizing the field and temperature axis to the zero-field T_{SP} we find essentially the same U/D phase boundary. This corresponds to the theoretical prediction of a universal SP phase diagram.[33,35] Indeed, the experimental U/D phase boundaries in both, pure and doped $CuGeO_3$, do agree well with the theoretical prediction. In an external field the D phase is observed up to a Lifshitz point (T_L, H_L) with transition temperatures $T_{SP}(0)$ $> T_L \simeq 0.77 T_{SP}(0)$ independent of doping. The solid line in Fig. 14, which apparently describes the data very well, is based on the theoretical treatment of Cross.[35,81] In summary, there is no evidence that doping significantly affects the U/D phase boundary. This phase boundary is determined by $T_{SP}(0)$ for both, homogeneous and doped SP systems.

The situation changes when investigating the phase boundaries to the incommensurate high-field phase which do

change upon doping. In the case of the temperature-driven U/I transition, the main difference concerns the meaning of the phase boundary. In doped $CuGeO_3$ this transition is much broader than the U/D transition, whereas the U/I transition remains sharp in pure $CuGeO_3$. This field-induced additional broadening systematically increases with doping (see Fig. 16 below). In the doped system there is not only a field-induced modulation of the low-temperature structure, but also a strong enhancement of disorder. The latter leads to a change from a rather well-defined SPT at low fields to a crossover phenomenon at high magnetic fields. Due to these qualitative differences of the phase boundaries for $x=0$ and $x=1.4\%$, respectively, it is difficult to judge whether the T_{SP} follow a universal curve. In reduced scales the field dependence of the midpoints of the broad anomalies for x $=1.4\%$, which are shown in Fig. 14, seems to be slightly larger than that of T_{SP} for $x=0$.

At the third phase boundary, i.e., the D/I transition, we also find clear differences between pure and doped $CuGeO_3$. As mentioned above the hysteresis changes systematically with increasing Zn concentration. The phase diagram in Fig. 14 reveals two other differences. Normalized to the corresponding $T_{SP}(H=0)$, the $H_{D/I}$ are larger for $x=1.4\%$ than for $x=0$, i.e., $H_{D/I}$ is less suppressed upon doping than T_{SP}. Moreover, the temperature dependence of the transition fields differs. In pure $CuGeO_3$ there is a local maximum of $H_{D/I}$ at $T \simeq 8$ K, which leads to sequences of sharp phase transitions as a function of temperature for magnetic fields of $H \simeq 12.5$ T (see Ref. 43), as, e.g., a re-entrance of the incommensurate modulation with decreasing T. The phase diagram shows that such D/I transitions with decreasing temperature do not occur for $x=1.4\%$ (and $x=0.66\%$ see Fig. 12). In the doped compounds none of our measurements, which were performed after cooling in the external field, reveals clear signatures of temperature-driven transitions between the D and I phases.

A local maximum of $H_{D/I}$, i.e., the sign change of $\partial H_{D/I}/\partial T$, implies that the entropy jump (ΔS) at the D/I transition changes sign at this temperature as well, since both quantities are related by the Clausius-Clapeyron relation

$$\frac{\Delta S}{\Delta M} \propto -\frac{\partial H_{D/I}}{\partial T}, \qquad (8)$$

where ΔM denotes the jump at the magnetization. This means that the different temperature dependences of $H_{D/I}$ in pure and doped $CuGeO_3$ are directly related to the qualitatively different jumps of the specific heat at $H_{D/I}$ (see Fig. 8 above). The increase of $H_{D/I}$ with decreasing T in doped $CuGeO_3$ shows again that in these systems the ''magnetic disorder'' as measured by the entropy always increases at the D/I transition in contrast to that of pure $CuGeO_3$. Thus, an enhancement of disorder when entering the I phase in doped compounds is not only signaled by the broadening of the U/I transition, but also causes small differences in the D/I phase boundary. This refers to the temperature dependence of $H_{D/I}$ but also to its absolute value, since the entropy affects the field dependence of the free energy (at fixed T). Thus, the increase of disorder at the D/I transition, occurring in doped compounds only, gives a plausible interpretation of the larger
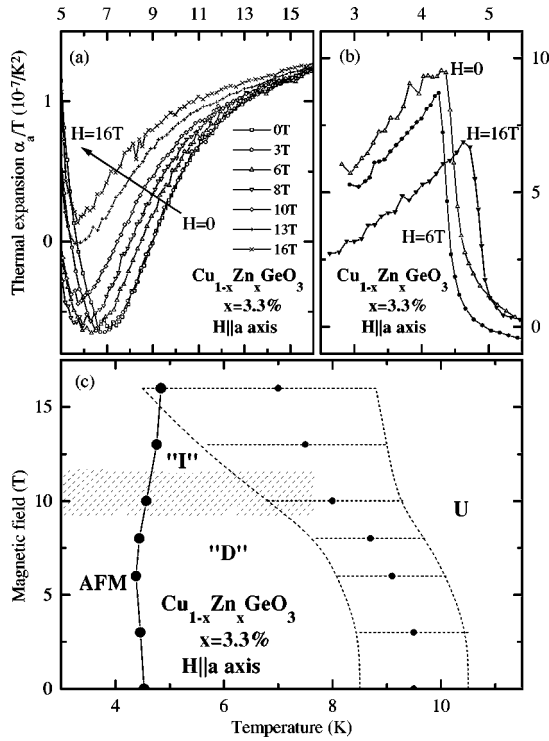
FIG. 15. Upper panel: Thermal expansion (α_a/T) of $Cu_{0.967}Zn_{0.033}GeO_3$ along the a axis for different magnetic fields. Left: Behavior at the crossover to the SP like state. Right: Anomaly of α_a at T_N. Lower panel: H,T phase diagram of $Cu_{0.967}Zn_{0.033}GeO_3$ as revealed from α_a, showing the field dependence of the well defined T_N at low temperatures and that of the broad crossover to the SP like state at higher temperatures. The hatched area marks the field range with the strongest field dependence of α (see text).

$H_{D/I}$, which we find when comparing the phase diagrams of doped and pure $CuGeO_3$ in reduced scales.

Summarizing the discussion of the D/I boundary, we find that defects are indeed important for details of this phase boundary, as suggested in several theoretical works.[74,2,36,37] The systematic changes of both the size and shape of the field hysteresis, give evidence for a pinning of the structural modulations at the doped defects as suggested in theoretical treatments. Moreover, an enhancement of disorder with *increasing field at fixed x* seems to be a further characteristic feature when entering the I phase of doped $CuGeO_3$. This causes differences to the findings in the pure compound, concerning a field dependent width of T_{SP}, the temperature dependence of $H_{D/I}$ and the absolute value of $H_{D/I}$ as well.

We turn now to our findings for the third Zn-doped sample with the highest concentration of $x=3.3\%$. This crystal does not show a sharp SPT even in $H=0$, but a broad crossover to a short-range dimerized phase. Applying a magnetic field further increases the width of the transition as shown in Fig. 15(a). Nevertheless, the characteristic field dependence of α, which is related to the suppression of the SPT, is still visible. The decrease of α_a starting at $T \simeq 11$ K for $H=0$ weakens with increasing H and shifts to lower temperatures. We have also measured a crystal with much higher effective doping (3% Si). In this crystal no hints on a SPT are found, i.e., there is no increase of α_a with increasing H (see Fig. 16 below). Thus, the field dependence
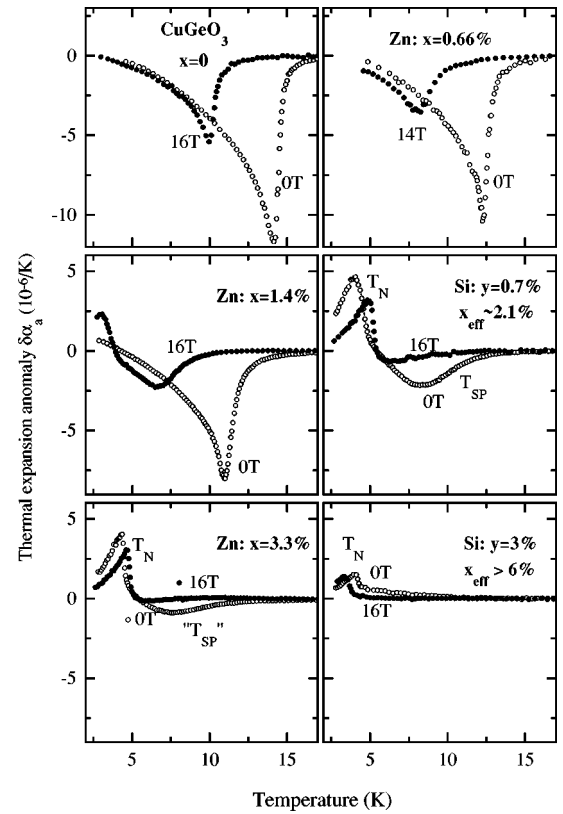

FIG. 16. Anomalies of the thermal-expansion coefficient α_a in zero field (open symbols) and in large magnetic fields (closed symbols) for different doping concentrations given in the figure. Note the different scale of the y axes in the two upper diagrams.

of α_a shown in Fig. 15(a) for the 3.3% Zn-doped crystal clearly shows remainders of the strongly suppressed SPT. Moreover, the field dependence of the thermal-expansion anomalies even reveals clear similarities to a SP phase diagram. As shown in Fig. 15(c), the midpoints of the broad transitions decrease from $\simeq 9.5$ K for $H=0$ to $\simeq 8$ K at $H = 10$ T. Surprisingly, this agrees with the field dependence which is predicted by the theoretical curve in Fig. 14 assuming a SPT at $T_{SP}(0)=9.5$ K, i.e., even the broad crossover seems to follow the prediction of Cross. Moreover, assuming this T_{SP}, one expects a change to the incommensurate phase for fields above 10 T. Again, the remainders of this change are clearly visible in the data for the $x=3.3\%$ crystal in Fig. 15(a). The anomaly at 13 T markedly differs from that at $H = 10T$. This concerns its size which is reduced and, in particular, its width, which is much larger in the higher field. The SP phase seems to disappear and, indeed, it is impossible to reveal a SPT from a single measurement in this high-field range. Its presence for $H = 13$ T is, however, inferred from the change of α when further increasing the magnetic field. This drastic suppression of the anomalies in the high-field range is not surprising, when taking into account our findings for the smaller Zn content of $x=1.4\%$. For $x = 3.3\%$ the broadening of the transition present already for $H=0$ T, adds with the additional broadening at high magnetic fields which is characteristic for doped $CuGeO_3$.

Turning back to the field dependence of α for $x=3.3\%$, the data in Fig. 15(a) reveal a quantitative change between $H \lesssim 10$ T and higher fields. However, in contrast with the

findings at lower doping it is not possible to extract a D/I phase boundary from the field dependence of the lattice constants. The corresponding magnetostriction measurements only show a continuous decrease of the lattice constant with some changes of the curvature which are related to the nonlinear field dependence of α. From these data it is neither possible to derive a qualitative difference between the high- and low-field range, nor to extract any meaningful phase boundary. We note that this holds also for a smaller effective doping of $x_{eff} = 2.1\%$ (0.7% Si). This latter finding compares well with diffraction measurements in high magnetic fields performed on a crystal with the same doping.[60] Instead of a splitting of the superstructure reflections due to an incommensurate modulation, which is found for $x = 0$ and smaller x_{eff},[40,60] there is only a pronounced broadening as a function of H. According to this finding, the high-field phase for $x_{eff} = 2.1\%$ corresponds rather to a short-range dimerized than to a long-range incommensurate phase.

Thus for the higher doping $x = 3.3\%$, both the $H = 0$ and the high-field phase should be regarded as short-range D phases. There is, however, still a decrease of the averaged SP order-parameter square $\langle A^2 \rangle$ as a function of H, which is most pronounced in the range of fields where the D/I transition takes place in a long-range ordered SP compound with the corresponding T_{SP}.

Whereas the SP instability does not lead to any phase transition in the thermodynamic sense in the crystal with a Zn doping of $x = 3.3\%$, a sharp phase boundary is present at $T \lesssim 5$ K, signaling long-range AFM order. The corresponding anomalies of the thermal expansion are shown for three representative magnetic fields in Fig. 15(b). Note that it is very easy to distinguish the AFM transition and the SP instability in the thermal expansion, since the signs of the corresponding anomalies differ. It is apparent from Fig. 15(b) that the magnetic field has only a small influence on the AFM order. The shape of the anomalies of α_a does not change significantly. There is, however, a small monotonous decrease of the $\Delta \alpha_a(T_N)$ with increasing field. Moreover, small changes of T_N are seen in the data in Fig. 15(b). For small fields, T_N slightly decreases with increasing H and, at $\simeq 6$ T, a minimum value of $T_N \simeq 4.4$ K is found which is about 0.15 K smaller than $T_N(H=0)$. With further increasing field, T_N increases again and the largest value, which amounts to $\simeq 4.8$ K, is found at $H = 16$ T. We mention that we obtain similar results for $x_{eff} \simeq 2.1\%$ (0.7% Si), which show, however, a slightly larger field dependence of T_N [$T_N(16$ T$) - T_N(0) \simeq 0.7$ K].

Though these field dependences of T_N are rather weak, the qualitative behavior compares well with that inferred above for $x = 1.4\%$. This concerns the nonmonotonous field dependence as well as the field range of the strongest changes which is close to the transition (crossover) to the high-field SP phase in all cases.

We emphasize that all above statements concerning the field dependence of the AFM order refer to magnetic fields applied parallel to the a axis of the crystals. For $H \| c$ the behavior is more complicated since there is a spin-flop transition for $H \lesssim 1.5$ T, which causes a minimum of $T_N(H)$ and slightly smaller T_N in high magnetic fields (see, also, Refs. 58,14,6). In the context of the present paper, this additional complication of the field influence on the AFM order is not

important. The field influence for $H \| a$ (and $H \| b$) as well as the changes as a function of doping described above, are also visible in our data for $H \| c$ besides the additional features due to the spin flop.

Before we further discuss our findings for the doped compounds in external fields, we shortly compare the presented phase diagrams to other studies of doped $CuGeO_3$ in external fields. The similarity of the SP phase diagrams to that for $x = 0$ was also revealed from magnetization measurements[59] and confirmed for both Si- and Zn-doped crystals in more detailed studies, using different experimental techniques (see, e.g., Refs. 58,45,46). However, two reported phase diagrams which are both based on ultrasound measurements contradict the systematic behavior presented here. The two studies, which were performed on a Zn-doped crystal with $x = 2\%$ by Saint-Paul et al.[57] and on a Si-doped crystal ($y = 0.7\%$, $x_{eff} \simeq 2.1\%$) by Poirier et al.,[56] reveal high-field phase boundaries which markedly differ from our findings. In this context it is, however, important to note that it is complicated to discriminate the AFM ordering and the SPT from the ultrasound measurements, since both cause a decrease of the elastic constant.

In order to explain a sharp phase transition which occurs below $\simeq 4.5$ K for $H \gtrsim 10$ T, Saint-Paul et al. introduce a new I' phase.[57] Moreover, in their phase diagram for $x = 2\%$ the I phase disappears at $H \gtrsim 15$ T. Based on our data, which allow to distinguish unambiguously between AFM and SP transitions, we suggest a reinterpretation of the anomalies visible in the elastic constant data. The sharp low-temperature anomaly is not due to a new I' phase but instead has to be attributed to T_N which increases for $H \gtrsim 10$ T as in our samples with larger and smaller x. The second difference, i.e., the disappearance of the I phase shown in the phase diagram of Saint-Paul et al., is not really inconsistent with our findings. The well-defined U/I phase boundary disappears already for a smaller Zn content of $x = 1.4\%$, which explains the absence of sharp features in high fields for $x = 2\%$. Using exactly the same arguments as above, it is also possible to explain the qualitative differences between the phase diagrams shown here and the phase diagram, Poirier et al. present for $x_{eff} \simeq 2.1\%$ (0.7% Si). In their work the sharp anomaly at the AFM order in high fields, which we clearly find in our crystal with the same stoichiometry, is attributed to the U/I transition.[56]

Following our suggestion and reinterpreting the sharp low-temperature anomalies of the elastic constants, leads to a rather consistent picture for the phase diagrams of doped $CuGeO_3$. In particular, at first glance rather surprising features of our data are consistent with other experimental studies. This concerns the strong additional broadening of the U/I phase boundary which can be extracted from the raw data presented in several studies.[45,46,56–58] Moreover, the pronounced increase of T_N for fields close to the D/I transition is (after the above reinterpretation) inferred from investigations for various (effective) defect concentrations.[45,46,56–58] This latter effect is most pronounced for crystals with a small (effective) doping, i.e., with a small T_N at $H = 0$, whereas at higher doping the field dependence of T_N is only small. Finally, we mention that, neither from the data on the Zn-doped crystals presented here, nor from our data on a Si-doped crystal with $y = 0.7\%$ ($x_{eff} \simeq 2.1\%$) do we find

evidence for an unusual AFM state at $H \sim 7$ T, which was recently reported in Refs. 45,46 for a Si-doped crystal with a smaller effective doping ($x_{eff} \sim 1.6\%$). However, note that this field corresponds roughly to the field with the minimum T_N in the compounds with higher doping. Moreover, the nonmonotonous field influence, which we observe for the Zn doping of $x = 1.4\%$ compares well to the findings of Sera *et al.*[46]

VI. DOPING AND FIELD DEPENDENCES: SIMILARITIES AND DIFFERENCES

The changes of the thermal expansion or the spontaneous strain in $Cu_{1-x}Zn_xGeO_3$ occurring as a function of field on the one hand and as a function of doping on the other, reveal some surprising similarities. This is displayed in Fig. 16, which compares α for $H = 0$ and large H measured on crystals with different defect concentrations. Here we show, in addition, data obtained on Si-doped compounds, in order to allow a more detailed discussion of the changes upon (effective) doping. It is apparent that both a large magnetic field as well as an increase of x_{eff} strongly suppress the size of the anomaly of α at T_{SP} and thus reduce the average SP order parameter square $\langle A^2 \rangle$. Note the qualitatively different field dependences of α for the highest (effective) doping (3% Si), which does not show any hint on a SPT. The small decrease of α_a in this crystal is probably due to the suppression of AFM correlations with increasing H and/or related to the field dependence of the doping-induced specific heat discussed above for $x = 1.4\%$.

Besides the reduction of $\langle A^2 \rangle$ there are two other striking similarities of the field and doping-induced changes of α_a. Increasing H as well as increasing x cause a change from a rather well defined SPT to a broad crossover. Moreover, the AFM transition appears in the accessible temperature range for both increasing H and increasing x. Before we discuss in detail these similarities, we emphasize that there are also clear differences between the field and doping influences. Such differences (and no meaningful similarities) are apparent when investigating properties which measure mainly the magnetic excitations as the specific heat (see, e.g., Fig. 8). But even if we restrict to α, field and doping act differently. Taking into account not only the shapes and sizes of the anomalies but also the transition temperatures, these differences are apparent from Fig. 16 as well. In zero field, there are no sharp phase transitions with sizeable $\Delta\alpha$ at transition temperatures well below 10 K. Such transitions do, however, occur in the high-field range (see, e.g., the data for $x = 0.66\%$). Similar sizes (and shapes) of $\Delta\alpha$ in high and low fields do not correspond to the same T_{SP}. Thus, a large magnetic field does not only increase the disorder, but also reduces T_{SP}. Vice versa, a strong reduction of $\Delta\alpha$ due to a large field does not necessarily imply a pronounced broadening of the transition. For $x = 0$ the anomalies at T_{SP} remain sharp even in the very large fields.[41] Thus, field and doping do not act identically and in order to understand the striking similarities in Fig. 16, we have to discuss separately the three observations indicating a relationship between field and doping dependences, which are (i) the reduction of $\langle A^2 \rangle$, (ii) the broadening of the SPT, and (iii) the increase of T_N.
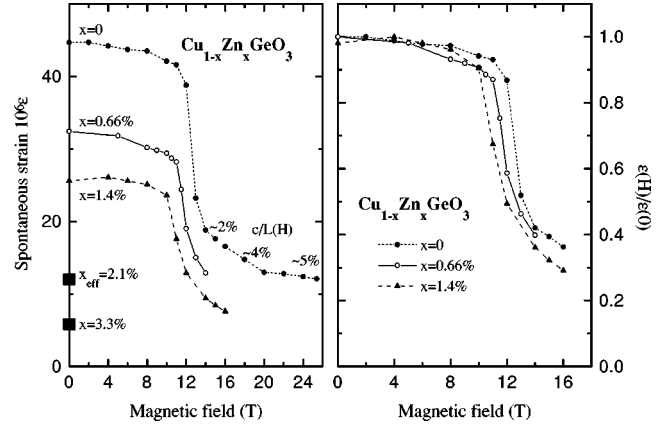

FIG. 17. Left: Magnetic-field dependence of the low-temperature spontaneous strain in $Cu_{1-x}Zn_xGeO_3$ ($x \lesssim 1.4\%$). For comparison, the $H = 0$ results for higher doping (——) are also shown. The $L(H)$ for $x = 0$ are extracted from magnetization data (Ref. 41). Right: Same data normalized to the zero field value.

A. Reduction of $\langle A^2 \rangle$ as a function of H and x

In Sec. III we have interpreted the reduction of the $H = 0$ spontaneous strains upon doping in terms of defect-induced solitons (see Fig. 3). Several experimental observations indicate that a soliton picture is also applicable when discussing the incommensurate modulation in $CuGeO_3$.[38-41] Actually, our above analysis uses the result of one of these studies, namely the determination of the correlation length ξ from x-ray-diffraction studies close to $H_{D/I}$.[38,40] This suggests that it is possible to describe both, $\langle A^2(x, H = 0) \rangle$ and $\langle A^2(x = 0, H) \rangle$, with Eq. (2) taking the same ξ. One then expects the same $\langle A^2 \rangle$, if the average distance of dopants equals the distance between nodes of the dimerization amplitude $L(H) = \pi/\Delta q(H)$ in the I phase, which is given by the modulation period $\Delta q(H)$.

Let us contrast this with the experimental observations. In Fig. 17 the field and doping dependences of $\langle A^2 \rangle$ are compared. For $x = 0$ we show data measured up to 25 T,[41] i.e., for a large range of $L(H)$. We have indicated the inverse distance of the order-parameter nodes $c/L(H)$ in the figure. In the case of doping, the corresponding quantity, i.e., the distance between solitons for $H = 0$, is given by the concentration x of Zn atoms. Comparing the data for $H = 0$ at different x with the field dependence at $x = 0$, clearly shows that $x \simeq c/L(H)$ does not imply the same squared SP order parameter. Only very close to the D/I phase boundary does a similar distance of order parameter nodes $[x \simeq c/L(H)]$ correspond to similar values of $\langle A^2(x = 0, H) \rangle$, on the one hand, and $\langle A^2(x, H = 0) \rangle$, on the other hand. However, at higher magnetic fields $\langle A^2(x = 0, H) \rangle$ saturates at a rather large value, though $L(H)$ becomes very small. Such a saturation at a finite $\langle A^2 \rangle$ is not observed for the reduction of $\epsilon(H = 0)$ upon doping.

This saturation of $\langle A^2(x = 0, H) \rangle$ contradicts Eq. (2) (Ref. 41) showing that a soliton description (with constant ξ) is not applicable in the I phase when considering a large range of $L(H)$. According to a recent theoretical study which is based on symmetry arguments, a multiplane-wave Ansatz of the form $A(x) = \Sigma a_m \cos(m\Delta qx)$ with $m = 1,3,5,\ldots$, i.e., a periodic modulation containing higher harmonics, is the gen-

eral description of the order parameter in the I phase of pure CuGeO$_3$.[73] Close to the D/I transition, the higher harmonics are important and a spatial modulation of the dimerization similar to a lattice of domain walls can occur. Indeed, if we limit ourselves to this field range, doping and field dependences of $\epsilon \propto \langle A^2 \rangle$ can be described in the same framework and, remarkably, the corresponding correlation lengths are in fair agreement (see Fig. 3). However, in general, there is a clear difference between field and doping dependences. Applying the soliton picture to the I phase at higher fields reveals much smaller ξ, which, moreover, systematically decrease with H. The main characteristics of the I phase (for $x=0$) is a *regular periodic* arrangement of order-parameter nodes with a field-dependent period. The spatial modulation of A changes continuously with increasing H and, finally, a simple sine-wave modulation with an H-independent amplitude is present.[41] In contrast, *real domain walls* exist in doped CuGeO$_3$ and the soliton picture reveals a reasonable description of the data (for $H=0$) also for small distances between the defects.

So far, we have compared the I phase of pure CuGeO$_3$ with the zero-field data of the doped compounds. The field-induced D/I transition also causes a drastic reduction of $\langle A^2 \rangle$ in doped CuGeO$_3$. For high doping, however, the anomalies of the thermal expansion at high fields are extremely small and, moreover, the low-temperature behavior is masked by the anomalies at the AFM transition. Therefore, it is impossible to extract meaningful values for $\epsilon(T \to 0)$ in this doping range. The corresponding data measured at small Zn concentrations are displayed in Fig. 17. There is no strong change of the field dependences of ϵ as a function of x for $x \leq 1.4\%$. The size of the reduction at the D/I transition decrease with increasing x. This is, however, a consequence of the reduced zero-field spontaneous strain only. Indeed, plotting the data on a normalized scale, i.e., dividing the $\epsilon(H)$ by the corresponding zero-field values, a nearly identical curve is obtained for $0 \leq x \leq 1.4\%$ as shown in the right part of Fig. 17. The remaining small differences are due to the slightly different $H_{D/I}$. Note that close to the phase boundary the period $\Delta q(H)$ depends on H and $(H-H_{D/I})$, whereas it is determined by H alone at higher fields.[35]

Ignoring these slight differences close to the phase boundary the scaling of $\epsilon(H)$ for different x means that field and doping dependences of $\langle A^2 \rangle$ at low temperatures (and small x) are given by

$$\langle A^2(x,H) \rangle \simeq \langle A^2(x,0) \rangle \langle A^2(0,H) \rangle \quad (\text{for } T \to 0). \quad (9)$$

The presence of *random* doping-induced domain walls is irrelevant for the suppression of $\langle A^2(T \to 0) \rangle$ which arises due to the *periodic* modulation of the dimerization in the high-field phase. Vice versa, Eq. (9) means that the incommensurate modulation of the dimerization is irrelevant when discussing the suppression of $\langle A^2(T \to 0) \rangle$ upon doping. Thus, it is possible to describe the suppression of the I phase order-parameter square in the same way as we did in Sec. III for the dimerization. The doping dependence of $\epsilon[T \to 0]$ in the I phase at a fixed $L(H)$ is obtained, if we replace the expression for the dimerization without defects $[(-1)^l A_0]$ by a more complicated one, containing the incommensurate modulation as, e.g., the multiplane-wave expression given

above. Describing the additional spatial modulation due to the doped defects for small x by $\tanh(lc/\xi)$ using the same ξ in both phases, does already explain our findings. This means that in both cases defects cause a suppression of the periodic distortions of the uniform lattice, which are present in the D as well as in the I phase.

In summary, investigating the averaged order-parameter square at low temperatures and for small x, does not reveal any relationship between doping-induced and field-induced modulations of the dimerization. Whereas an increase of x indeed corresponds to a larger number of solitons, the field-induced D/I transition should be regarded as a change of the underlying undistorted lattice. Nevertheless, a relationship between field and doping dependences is revealed from our thermal-expansion data. For example, the U/I transitions and the temperature dependences of $\langle A^2 \rangle$ markedly differ in pure and doped CuGeO$_3$, respectively. A separation of x and H dependences in terms of Eq. (9) is impossible at higher temperatures. Moreover, Fig. 16 indicates similarities concerning the x and H dependences of the AFM transition. However, the considerations in this section show that one clearly has to discriminate between *random* domain walls due to doped defects, on the one hand, and *periodic* order parameter nodes due to a large magnetic field on the other. In the latter case the soliton picture is not applicable when considering a larger range of magnetic fields.

B. From long-range to short-range order as a function of H and x

The pronounced broadening of the U/I transitions in doped CuGeO$_3$ is a very surprising feature revealed by our data. Usually a broad phase transition is attributed to sample inhomogeneities, in particular in a doped compound. However, in the present case the zero- and low-field data on the same crystals clearly show the homogeneity of the samples at least for small x. It is therefore necessary, to find a physical origin of the pronounced broadening of the phase transitions in high magnetic fields.

Let us start the discussion of this field-induced broadening by investigating the pure compound. Neither the data shown in Fig. 16 nor the thermal-expansion measurements in even higher fields up to 28 T (Ref. 41) yield any evidence for an increase of the transition width with H. A small broadening of the thermal-expansion anomaly is only found close to the Lifshitz point due to the enlarged fluctuation regime,[73] but with further increasing H, the anomaly sharpens again.[43,41] Thus, any explanation of the broad U/I boundary has to include both a high magnetic field $H > H_{D/I}$ and a finite x.

The effects of disorder on the D and I phases have been considered recently by Bhattacharjee *et al.* in their theoretical study.[73] The random substitutions are modeled by randomness in the coefficients of the original Landau Hamiltonian, which describes phenomenologically the U/I and U/D transitions. It is indeed found that the effect of disorder is more severe in the I than in the D phase. The defects do not only suppress locally the amplitude of the order parameter as in the D phase. In addition the random impurity positions cause a random phase of the incommensurate modulation. According to Bhattacharjee *et al.* this latter randomness destroys the true long-range order of the I phase.[73] For small

impurity concentrations there is, however, still quasi-long-range order, which explains the presence of Bragg peaks for small x.[40,60] Note that the phase randomness is not crucial for the averaged SP order-parameter square, which we have discussed above, and therefore the additional disorder does not strongly modify the field dependence of $\langle A^2 \rangle$ at low T and x.

It is, however, straightforward to attribute the additional broadening of the thermal-expansion anomalies for $H > H_{D/I}$ to this additional influence of disorder. The absence of true long-range order does qualitatively explain the absence of a true U/I phase transition in the thermodynamic sense, which is signaled by our data already for moderate doping. Since the incommensurate modulation is essential for the above arguments, it is also apparent that the U/I transitions are much broader than the U/D transitions of the same sample. As discussed above, an enhancement of disorder when entering the I phase as a function of H, explains in addition the differences observed for the D/I phase boundary in doped and pure $CuGeO_3$.

The presented interpretation of the additional broadening of the SPT in large fields is based on the qualitative change of the structural distortion at $H_{D/I}$. Though this does not occur as a function of x at $H=0$, a qualitatively similar broadening of the SPT as a function of x may occur, since the origin of the disorder is not crucial in this respect. This explains the corresponding similarity between x and H dependences of the thermal-expansion data in Fig. 16. In order to understand the similarity concerning the changes of T_N, we have to expand our discussion which, so far, has only considered the structural order parameter.

C. Competing spin-Peierls and antiferromagnetic order

It is well known that long-range Néel ordering and the SPT are competing phenomena in quasi-one-dimensional antiferromagnets. Theoretical treatments for homogeneous systems show that AFM order and SPT mutually exclude each other.[32,29] The situation changes for a disordered SP system. Néel order and SPT still compete, but now the theoretical studies yield also the coexistence of both ordering phenomena in agreement with the experimental studies on doped $CuGeO_3$.[21–23,29] Recently, Mostovoy *et al.* analyzed the (x,T) phase diagram of disordered SP systems[29] and we will use some of their results as a starting point for a phenomenological interpretation of the field dependences of T_N in doped $CuGeO_3$.

Mostovoy *et al.* consider a Landau expansion of the free energy of the form

$$\Delta F = a_{SP}[T - T_{SP}^0(x)]\langle A^2 \rangle + \frac{b_{SP}}{2}\langle A^2 \rangle^2$$
$$+ a_{AFM}[T - T_N^0(x)]A_{AFM}^2 + \frac{b_{AFM}}{2}A_{AFM}^4 + c\langle A^2 \rangle A_{AFM}^2, \tag{10}$$

where A and A_{AFM} denote the SP and AFM order parameters, respectively. T_{SP}^0 and T_N^0 are the bare ordering temperatures, which represent the doping dependences without a coupling between SP and AFM order parameters. The signs of the constants $a_{SP}, a_{AFM}, b_{SP}, b_{AFM} > 0$ and $c^2 - b_{SP}b_{AFM} < 0$ are

given from the required stability of the system. Mostovoy *et al.* use this expansion to derive the phase diagram near a multicritical point with $T_N(x) = T_{SP}(x)$, where the consideration of these leading orders of the free-energy expansions suffices. The competition between SP and Néel states is described by the last term in Eq. (10), which couples the SP and AFM order parameters. As a consequence T_N depends on the dimerization

$$T_N(x) = T_N^0(x) - \frac{c}{a_{AFM}}\langle A^2(T_N) \rangle, \tag{11}$$

and for $c > 0$ dimerization suppresses the AFM state, i.e., T_N decreases with increasing $\langle A^2 \rangle$. Vice versa, the same coupling term implies that the dimerization decreases when A_{AFM}^2 becomes finite below T_{SP}. Minimizing e.g., Eq. (10) with respect to A yields

$$\langle A^2 \rangle = \frac{a_{SP}}{b_{SP}}[T_{SP}^0(x) - T] - \frac{c}{b_{SP}}A_{AFM}^2 \tag{12}$$

for $T < T_{SP}$. Consequently, a rich phase diagram is derived from Eq. (10), showing, e.g., a re-entrance into an undimerized state in some regions of disorder strength.[29]

As revealed by the experiments on doped $CuGeO_3$, the situation in the real system is more complicated. Already for moderate doping there is a change from a SPT to a short-range order phenomenon. The assumption $T_{SP} \sim T_N$ underlying the free-energy expansion in Eq. (10) is not realized. Nevertheless, features predicted from Eq. (10) are clearly found in the experiment. For example, it is apparent from Fig. 16 that the anomaly of α at T_N is much larger at doping with finite dimerization than for a Si content of $y = 3\%$. On the other hand, this latter crystal exhibits the largest specific-heat anomaly at T_N (see also similar results in Ref. 45), showing that the smaller $\Delta\alpha$ is not related to the AFM order parameter. The origin of the larger $\Delta\alpha$ in the case of coexisting SP and AFM transitions is apparent from Eq. (12). There is an additional contribution due to the decrease of the dimerization. Note that this contribution straightforwardly explains the anticorrelation of the signs of the thermal-expansion anomalies at T_{SP} and T_N, respectively, which we find in all crystals and along all three lattice directions.

However, a quantitative analysis of our data in terms of Eq. (12), i.e., the determination of the decrease of $\langle A^2 \rangle$ due to AFM order, is impossible. On the one hand, it would be necessary to introduce several parameters, in order to describe $\langle A^2(T) \rangle$ for temperatures well below T_{SP}, since the leading orders in Eq. (10) are not sufficient. On the other hand, there is also a significant direct coupling between lattice strains and the AFM order parameter.[82] This latter contribution is not only visible for the highly doped crystals with $\langle A^2 \rangle \simeq 0$. It is also inferred when comparing quantitatively the large decrease of ϵ at T_N with the results from neutron-diffraction studies which reveal only a moderate decrease of the dimerization, i.e., of the intensity of the superstructure reflections at T_N.[18,12,20,15]

Therefore we restrict the following discussion to the changes of T_N and will not consider the implications of the AFM order for the dimerization. The SP order parameter is taken as an input parameter and the consequences for T_N are
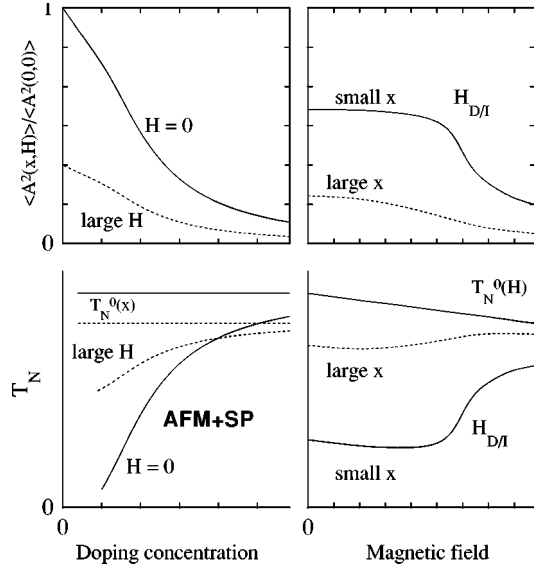
FIG. 18. Schematic illustration of the changes of T_N due to the coupling between SP and AFM order parameters. In the two upper figures representative x (left) and H (right) dependences of $\langle A^2(x,H) \rangle$ are sketched. In the two lower figures the corresponding changes of T_N obtained from Eq. (11) are depicted. For the illustration we assume $\partial T_N^0(x,H)/\partial x = 0$, $\partial \ln T_N^0(x,H)/\partial H = -0.88\%/T$, and an H and x independent coupling of $\partial T_N/\partial \langle A^2 \rangle = -1.2 T_N^0(x,0)/\langle A^2(0,0) \rangle$ (see text).

described with Eq. (11). Such a treatment is not only possible for $T_N \simeq T_{SP}$ considered by Mostovoy *et al.*, but also for $T_N \ll T_{SP}$. The result for $H=0$ is sketched by the solid lines in Fig. 18. In the upper panel a concentration dependence of $\langle A^2 \rangle$ is depicted which corresponds to our findings at low temperatures $T \ll T_{SP}$ (see Fig. 3). In the lower panel, the corresponding concentration dependence of T_N as determined from Eq. (11) is shown. In this schematic representation we assume for simplicity a concentration-independent $T_N^0(x)$ which then corresponds to T_N for very large x with $\langle A^2 \rangle \simeq 0$. Due to the increase of the SP order parameter, T_N decreases with decreasing x and disappears when the suppression due to the dimerization exceeds the bare T_N^0. Note that a similar $H=0$ phase boundary is obtained from the calculations of Mostovoy *et al.*, which take into account in addition the temperature dependence of $\langle A^2 \rangle$ as derived from Eq. (10) and a slight decrease of $T_N^0(x)$ with increasing x.[29]

Let us now qualitatively discuss our findings as a function of H in a framework similar to Eq. (10). In particular, we take the same expression for the coupling term. To include the magnetic field in the free-energy expansion describing the AFM order is straightforward. We replace the bare concentration dependence $T_N^0(x)$ by a bare field dependence $T_N^0(H)$.[83] An estimate for this bare field dependence can be taken from the Si-doped crystal with $y=3\%$. In this crystal with $\langle A^2 \rangle \simeq 0$, T_N decreases monotonously by $\simeq 0.6$ K/16 T with increasing H. Equation (11) yields an additional field dependence for compounds with coexisting SP and AFM order which arises from the suppression of the SP order parameter $\langle A^2(H,x,T_N) \rangle$ with increasing H. Correspondingly, the total field dependence of T_N has two contributions with opposite signs: a small decrease with increasing

H, representing the bare $T_N^0(H)$, and an increase due to the reduction of $\langle A^2 \rangle$ in large magnetic fields.

This behavior is sketched in the right part of Fig. 18. In the upper panel we show for two representative concentrations the field dependence of $\langle A^2 \rangle$, using the same scales as in the left part of the figure. The field dependence of T_N which is then derived according to Eq. (11) is shown in the lower part of the figure. The result fits surprisingly well with our experimental observations. For small fields there is no significant H dependence of $\langle A^2 \rangle$ at $T \simeq T_N$ (see, e.g., Fig. 17) and $T_N(H)$ is determined by the decrease of $T_N^0(H)$. This suppression of T_N as a function of H was inferred above from the data for $x=1.4\%$ and observed for the higher concentrations. The coupling between AFM and SPT becomes very important for magnetic fields close to the D/I transition, which causes a strong decrease of $\langle A^2 \rangle$ (for small x). In this field range we therefore expect a rather strong increase of T_N as we observe for $x=1.4\%$ and as reported in the literature for crystals with similar effective doping.[58,45,46,56,57] We note that in our description T_N is not influenced by a hypothetical $\langle A^2(T=0) \rangle$ which is nearly field independent for $H < H_{D/I}$.[43] Instead we have to consider $\langle A^2 \rangle$ at T_N. Due to the decrease of T_{SP} with H, this quantity does already change for fields significantly below $H_{D/I}$ (see the data in Fig. 6), in particular, if the zero field T_{SP} is already reduced due to doping. Correspondingly, the minimum T_N occurs not directly at, but below $H_{D/I}$.

The different amount of the increase of T_N which we observe for different compositions follows straightforwardly in the same way. For low concentrations, the zero field $\langle A^2 \rangle$ is still rather large, which implies a drastic decrease as a function of field (see Fig. 17). In absolute units this field dependence is much weaker for higher doping. Thus, at low doping Eq. (11) predicts a much larger increase of T_N at the D/I transition than for larger x. These x-dependent field influences on T_N obviously mean that the (x,T) phase diagrams at zero and large fields markedly differ with respect to the AFM phase. This is also sketched in the left part of Fig. 18. The concentration dependence of T_N is much weaker in high fields than in zero field, since the concentration dependence of $\langle A^2 \rangle$ is smaller in absolute scales (see upper part of Fig. 18).

For large x, AFM order is suppressed by a large field due to the decrease of $T_N^0(H)$. With decreasing x the zero and high-field phase boundaries cross and, at intermediate and low doping, a high field enhances AFM order. Equivalently, the difference of zero- and high-field T_N systematically decreases with increasing x. This is clearly found in the experiments. According to our data the difference $T_N(16T) - T_N(0)$ amounts to $\gtrsim 1.5$, 0.7, and 0.3 K for $x=1.4\%$, $x_{eff} \simeq 2.1\%$, and $x=3.3\%$, respectively, and, finally, at the largest effective doping ($y=3\%$), T_N decreases with H.

We conclude that the observed H dependences of T_N as well as their systematic changes upon doping are reproduced, if we assume a coupling of SP and AFM order parameters in terms of Eqs. (10) and (11). This is shown in the two schematic figures in the lower part of Fig. 18. Here we use a coupling constant which neither depends on x nor on H. Moreover, we assume a bare T_N which does not depend on x

and decreases slightly with H, as observed at high doping. Remarkably, these most simple assumptions suffice to obtain a good qualitative agreement with the experiment, indicating that $T_N(x,H)$ is indeed determined to a large extent by the corresponding changes of $\langle A^2 \rangle$. It is worthwhile mentioning that in our description the origin of the changes of $\langle A^2 \rangle$ is irrelevant. A qualitative agreement with the data is already obtained, if we treat identically the reduction of $\langle A^2 \rangle$ due to solitonlike defects upon doping, on the one hand, and that due to the field-induced modulation of A on the other. This leads to the striking similarity of the x and H dependences of the thermal expansion (Fig. 16), which measures simultaneously both T_N by the corresponding anomaly as well as $\langle A^2 \rangle$ by the size of the anomaly at the SPT.

So far, we have only discussed qualitatively the coupling between SP and AFM order parameters. In principle, thermal-expansion data allow also a quantitative determination of the coupling strength in Eq. (11). However, the error of the coupling strength, as extractable from our present data, is rather large. On the one hand, we cannot follow $T_N(H)$ at low doping due to the restricted temperature range of our measurements. On the other hand, the field dependences of T_N and $\langle A^2 \rangle$ are rather small at high doping. This not only causes large relative errors, in addition, the bare field dependence and the coupling to $\langle A^2 \rangle$ are of comparable significance for $T_N(H)$ in this doping range and therefore the assumption for $T_N(H)$ strongly influences the result for the coupling strength. Within the limitations due do these uncertainties, our data are consistent with a field and concentration-independent coupling between SP and AFM order parameters. This coupling constant is not very large. Taking the $T \rightarrow 0$ dimerization of pure $CuGeO_3$, we estimate a suppression of T_N between 5 and 8 K, from the field dependences of T_N and Eq. (11). This value is comparable to the maximum T_N observed in doped $CuGeO_3$. Thus, our description suggests an AFM phase occurring already for very small x in agreement with recent experiments.[14,16]

In the context of this section it is worthwhile to mention a very recent study of Mg-doped $CuGeO_3$.[10] Based on susceptibility measurements it is argued that the SP order parameter vanishes abruptly at $z \simeq 2.3\%$ ($x_{eff} \simeq z$). According to Ref. 10 this is accompanied by an abrupt increase of T_N by $\simeq 0.8$ K. This correlation between jumplike changes of T_N and $\langle A^2 \rangle$ is qualitatively (and within the large error bars even quantitatively) consistent with our description. However, studies of $\langle A^2(z) \rangle$ in Mg-doped $CuGeO_3$ are desirable in order to confirm the absence of a short-range order SP-like state for $z > 2.3\%$, i.e., a pronounced difference between Zn and Mg doping in this respect. On the other hand, a detailed investigation of the coupling between SP and AFM order parameters would be possible. For example, our description predicts a sign change of the high field $\partial T_N / \partial H$ accompanied by the abrupt vanishing of $\langle A^2 \rangle$.

There is a further extension of our measurements suggested by the systematic behavior of $T_N(H,x)$ for $x_{eff} \gtrsim 1.4\%$. Extrapolating the observed doping dependence and/or applying our phenomenological description to smaller doping, we expect strong increases of T_N for magnetic fields $H \gtrsim H_{D/I}$. Thus, our description predicts that the minimum doping x_m showing AFM order significantly decreases in a large field (see Fig. 18). However, x_m is already very small

for $H = 0$. We, therefore, expect that the systematic behavior of $T_N(H,x)$, which we find at intermediate and large doping, markedly changes at low concentrations. One may, for example, speculate that the change from a quasi-long-range to a long-range ordered I phase with decreasing x (see above) also modifies the coupling between AFM and SP order-parameters in large fields.

VII. SUMMARY AND CONCLUSIONS

We have presented a comprehensive study of the thermodynamic properties thermal expansion, specific heat, and magnetostriction for a series of $Cu_{1-x}Zn_xGeO_3$ single crystals. With increasing defect concentration we find a drastic reduction of the averaged SP order parameter square $\langle A^2 \rangle$ which is consistent with the development of solitonlike defects. The correlation length which is obtained from a quantitative description of $\langle A^2(x) \rangle$ agrees well with that reported for the I phase of pure $CuGeO_3$ ($\simeq 13.6c$). Besides the reduction of the average SP order parameter, there is a drastic increase of the magnetic specific heat at low temperatures. Features due to singlet triplet excitations with a reasonable value of the spin gap are still found. However, C_{mag} at low temperatures is clearly dominated by low-energy excitations which arise upon doping. We have shown that the corresponding specific heat changes only weakly with T for 2.2 K $\lesssim$ T $\lesssim$ 5 K, but drastically reduces with increasing H. A possible interpretation in terms of disordered AFM chains is presented which agrees qualitatively with theoretical predictions for disordered SP systems.

The decrease of $\langle A^2 \rangle$ at low temperatures upon doping correlates with that of T_{SP} and the relationship between these two quantities is identical for Zn and Si-doped $CuGeO_3$. Doping suppresses $\langle A^2 \rangle$ much stronger than T_{SP} and for low doping ($x_{eff} \lesssim 2.1\%$) a scaling $\langle A^2(T \simeq 0) \rangle \propto T_{SP}^3$ is derived from our data. This observation for doped SP systems corresponds to the theoretical results obtained for homogeneous SP compounds. The soliton picture with $\xi \simeq 13.6c$ and this scaling corresponds to a nearly linear decrease of T_{SP} at small x which amounts to $\Delta T_{SP}/T_{SP} \simeq 15x$ as observed experimentally.

At higher doping the situation changes. While the susceptibility signals a disappearance of the SPT, our data indicate a change from a well-defined SPT to a crossover phenomenon with increasing x. The characteristic temperature of the latter remains high, though the SP order parameter becomes very small. A SP-like state is also present for rather high Zn doping ($x = 3.3\%$). At this high doping there is, however, neither a SPT in the thermodynamic sense, nor a well-defined phase boundary in the (x,T) phase diagram of $Cu_{1-x}Zn_xGeO_3$.

From our measurements in high magnetic fields we have also derived the influence of defects on the structural modulation of the I phase. Considering $\langle A^2(T \simeq 0) \rangle$ for small x, the reduction upon doping is very similar for the D and I phases. In this doping (and temperature) range we do not find any evidence for a connection between doping-induced solitons and the field-induced modulation of the structure.

Concerning the (H,T) phase diagrams our measurements reveal several systematic changes upon doping. These changes are small for the phase boundaries related to the

SPT. However, a universal SP phase diagram is only found for the U/D transition in doped $CuGeO_3$. This phase boundary is identical for crystals with different x after dividing both field and temperature axis by $T_{SP}(H=0)$, and, moreover, agrees well with the theoretical predictions. In contrast to that, all phase boundaries to the I phase do change upon doping. Most of these doping dependences can be straightforwardly interpreted, when taking into account an increase of disorder in this high-field phase. This additional disorder is a consequence of a random order-parameter phase which is only relevant in the I phase. This explains qualitatively that the anomalies at the U/I transitions are much broader than those at the U/D transitions in the same crystal. Moreover, enhanced disorder in the I phase could also give rise to the slight increase of the transition fields $H_{D/I}$ with increasing x which we observe when plotting the data in normalized scales. Finally, the enhancement of disorder at the field-induced transition from the D to the I phase at finite x explains that doped and pure $CuGeO_3$ exhibit qualitatively different temperature dependences of $H_{D/I}$ or, equivalently, different signs of the entropy jumps at $H_{D/I}$ at low temperatures. In addition, we find a systematic doping-dependent change of the hysteresis of the D/I transition. At low temperatures $\Delta H_{D/I}$ increases with x which indicates a pinning of the incommensurate modulation due to defect-induced disorder. However, the opposite trend is found at high temperatures. The temperature range, showing a clear hysteresis of transition fields, systematically decreases with increasing doping and the signatures of the first order D/I transitions disappear already for a moderate doping $x_{eff} \simeq 2.1\%$. A possible origin is again the H-dependent enhancement of disorder at the D/I transition, since at high temperature and/or high doping there is neither true long-range nor quasi-long-range order in the I phase of doped $CuGeO_3$.

Pronounced systematic changes upon doping are revealed in the (H,T) phase diagrams with respect to the AFM order. At very high doping with completely suppressed SPT, there is a small monotonous decrease of T_N. All crystals with finite $\langle A^2 \rangle$ show a nonmonotonous field dependence of T_N.

At small fields, AFM order is suppressed, whereas at higher fields an increase of T_N is observed. The minimum T_N is observed below the D/I phase boundary, but the changes are most pronounced for $H \simeq H_{D/I}$. Moreover, the amount of the increase of T_N systematically increases with decreasing doping. We have shown that assuming a coupling between SP and AFM order parameters can simultaneously describe this field dependence of T_N, its systematic change upon doping, as well as the concentration dependence of T_N at $H=0$.

Several issues raised in this paper could be further clarified by additional studies, both theoretically and experimentally. At present it is not clear to which extent the interchain coupling affects the spatial modulation of the dimerization due to the solitonlike defects. Moreover, we cannot judge from our present data, whether the short-range SP-like phase in $Cu_{1-x}Zn_xGeO_3$ at large doping $x \gtrsim 3\%$ is a property of a compound with random defects or related to local variations of the Zn content. Further studies for other x and other dopants could clarify this issue. Further systematic studies are also desirable in order to understand the behavior of the specific heat in doped $CuGeO_3$. This refers to the doping-induced excitations visible at low temperatures but also to the strong suppression and broadening of the anomaly at T_{SP} in moderate external fields $H < H_{D/I}$. Finally, an extension of our study of $T_N(H)$ to smaller doping and lower temperatures would be very interesting. Probably the systematic behavior of $T_N(H,x)$, which is the basis of the phenomenological description presented here, changes markedly when decreasing the doping. The rather large T_N at high fields which are extrapolated for small x from our findings are very unlikely to occur.

[1] M. Hase, I. Terasaki, and K. Uchinokura, Phys. Rev. Lett. **70**, 3651 (1993).

[2] For a review, see, J. W. Bray, L. V. Interrante, I. S. Jacobs, and J. C. Bonner, in *Extended Linear Chain Compounds*, edited by J. S. Miller (Plenum, New York, 1983).

[3] J. P. Boucher and L. P. Regnault, J. Phys. I **6**, 1939 (1996).

[4] J. P. Renard, K. Le Dang, P. Veillet, G. Dhalenne, A. Revcolevschi, and L. P. Regnault, Europhys. Lett. **30**, 475 (1995).

[5] M. Hase, N. Koide, K. Manabe, Y. Sasago, K. Uchinokura, and A. Sawa, Physica B **215**, 164 (1995).

[6] B. Grenier, J.-P. Renard, P. Veillet, C. Paulsen, R. Calemczuk, G. Dhalenne, and A. Revcolevschi, Phys. Rev. B **57**, 3444 (1998).

[7] S. B. Oseroff, S-W. Cheong, B. Aktas, M. F. Hundley, Z. Fisk, and L. W. Rupp, Jr., Phys. Rev. Lett. **74**, 1450 (1995).

[8] J-G. Lussier, S. M. Coad, D. F. McMorrow, and D. McK Paul, J. Phys.: Condens. Matter **7**, L735 (1995).

[9] M. Weiden, W. Richter, R. Hauptmann, C. Geibel, and F. Steglich, Physica B **233**, 153 (1997).

[10] T. Masuda, A. Fujioka, Y. Uchiyama, I. Tsukada, and K. Uchinokura, Phys. Rev. Lett. **80**, 4566 (1998).

[11] Y. Sasago, N. Koide, K. Uchinokura, M. C. Martin, M. Hase, K. Hirota, and G. Shirane, Phys. Rev. B **54**, R6835 (1996).

[12] M. C. Martin, M. Hase, K. Hirota, G. Shirane, Y. Sasago, N. Koide, and K. Uchinokura, Phys. Rev. B **56**, 3173 (1997).

[13] P. E. Anderson, J. Z. Liu, and R. N. Shelton, Phys. Rev. B **57**, 11 014 (1997).

[14] B. Grenier, J.-P. Renard, P. Veillet, C. Paulsen, G. Dhalenne, and A. Revcolevschi, Phys. Rev. B **58**, 8202 (1998).

[15] S. Katano, O. Fujita, J. Akimitsu, N. Nishi, K. Kakurai, and Y. Fushi, Phys. Rev. B **57**, 10 280 (1998).

[16] K. Manabe, H. Ishimoto, N. Koide, Y. Sasago, and K. Uchinokura, Phys. Rev. B **58**, R575 (1998).

[17] N. Koide, Y. Uchiyama, T. Hayashi, Y. Sasago, K. Uchinokura, K. Manabe, and H. Ishimoto, cond-mat/9805095 (unpublished).

[18] L. P. Regnault, J. P. Renard, G. Dhalenne, and A. Revcolevschi, Europhys. Lett. **32**, 579 (1995).

[19] K. M. Kojima, Y. Fudamoto, M. Larkin, G. M. Luke, J. Merrin, B. Nachumi, Y. J. Uemura, M. Hase, Y. Sasago, K. Uchinokura, Y. Ajiro, A. Revcolevschi, and J.-P. Renard, Phys. Rev. Lett. **79**, 503 (1997).

[20] K. Hirota, M. Hase, J. Akimitsu, T. Masuda, K. Uchinokura, and G. Shirane, J. Phys. Soc. Jpn. **67**, 645 (1998).

[21] H. Fukuyama, T. Tanimoto, and M. Saito, J. Phys. Soc. Jpn. **65**, 1182 (1996).

[22] D. Khomskii, W. Geertsma, and M. Mostovoy, Czech. J. Phys. **46**, Suppl. S6, 3239 (1996).

[23] M. V. Mostovoy and D. I. Khomskii, Z. Phys. B **103**, 209 (1997).

[24] G. M. Martins, E. Dagotto, and J. A. Riera, Phys. Rev. B **54**, 16 032 (1996).

[25] M. Fabrizio and R. Mélin, Phys. Rev. Lett. **78**, 3382 (1997).

[26] G. M. Martins, M. Laukamp, J. Riera, and E. Dagotto, Phys. Rev. Lett. **78**, 3563 (1997).

[27] M. Fabrizio and R. Mélin, Phys. Rev. B **56**, 5996 (1997).

[28] M. Laukamp, G. M. Martins, C. Gazza, A. Malvezzi, E. Dagotto, P. M. Hansen, A. C. López, and J. Riera, Phys. Rev. B **57**, 10 755 (1998).

[29] M. Mostovoy, D. Khomskii, and J. Knoester, Phys. Rev. B **58**, 8190 (1998).

[30] P. Hansen, D. Augier, J. Riera, and D. Poilblanc, cond-mat/9805325 (unpublished).

[31] M. Fabrizio and R. Melin, cond-mat/980793 (unpublished).

[32] S. Inagaki and H. Fukuyama, J. Phys. Soc. Jpn. **52**, 2504 (1983); **52**, 3620 (1983); **53**, 4386 (1984).

[33] L. N. Bulaevskii, A. I. Buzdin, and D. I. Khomskii, Solid State Commun. **27**, 5 (1978).

[34] M. Cross and D. S. Fisher, Phys. Rev. B **19**, 402 (1979).

[35] M. C. Cross, Phys. Rev. B **20**, 4606 (1979).

[36] T. Nakano and H. Fukuyama, J. Phys. Soc. Jpn. **49**, 1679 (1980).

[37] T. Nakano and H. Fukuyama, J. Phys. Soc. Jpn. **50**, 2489 (1981).

[38] V. Kiryukhin and B. Keimer, Phys. Rev. B **52**, R704 (1995).

[39] Y. Fagot-Revurat, M. Horvatić, C. Berthier, P. Sigransan, G. Dhalenne and A. Revcolevschi, Phys. Rev. Lett. **77**, 1861 (1996).

[40] V. Kiryukhin, B. Keimer, J. P. Hill, and A. Vigliante, Phys. Rev. Lett. **76**, 4608 (1996).

[41] T. Lorenz, B. Büchner, P.H.M. van Loosdrecht, F. Schönfeld, G. Chouteau, A. Revcolevschi, and G. Dhalenne, Phys. Rev. Lett. **81**, 148 (1998).

[42] T. W. Hijmans, H. B. Brom, and L. J. de Jongh, Phys. Rev. Lett. **54**, 1714 (1985).

[43] T. Lorenz, U. Ammerahl, T. Auweiler, B. Büchner, A. Revcolevschi, and G. Dhalenne, Phys. Rev. B **55**, 5914 (1997).

[44] U. Ammerahl, T. Lorenz, B. Büchner, A. Revcolevschi, and G. Dhalenne, Z. Phys. B **102**, 71 (1997).

[45] M. Hiroi, T. Hamamoto, M. Sera, H. Nojiri, N. Kobayashi, M. Motokawa, O. Fujita, A. Ogiwara, and J. Akimitsu, Phys. Rev. B **55**, R6125 (1997).

[46] M. Sera, K. Yamamoto, M. Hiroi, N. Kobayashi, O. Fujita, A. Ogiwara, and J. Akimitsu, Phys. Rev. B **56**, 14 771 (1997).

[47] S. Sahling, G. Remenyi, J. C. Lasjaunias, N. Hegmann, G. Dhalenne, and A. Revcolevschi, Physica B **219&220**, 110 (1996).

[48] X. Liu, J. Wosnitza, H.v. Löhneysen, and R. K. Kremer, Z. Phys. B **98**, 163 (1995).

[49] H. Winkelmann, E. Gamper, B. Büchner, M. Braden, A. Revcolevschi, and G. Dhalenne, Phys. Rev. B **51**, 12 884 (1995).

[50] T. Lorenz, U. Ammerahl, R. Ziemes, B. Büchner, A. Revcolevs-

[51] chi, and G. Dhalenne, Phys. Rev. B **54**, R15 610 (1996).

K. Fabricius, A. Klümper, U. Löw, B. Büchner, G. Dhalenne, T. Lorenz, and A. Revcolevschi, Phys. Rev. B **57**, 1102 (1998).

[52] S. Sahling, J. C. Lasjaunias, P. Monceau, and A. Revcolevschi. Solid State Commun. **92**, 423 (1994).

[53] T. Lorenz, H. Kierspel, S. Kleefisch, B. Büchner, E. Gamper, A. Revcolevschi, and G. Dhalenne, Phys. Rev. B **56**, 501 (1997).

[54] M. Fischer, P.H.M. van Loosdrecht, G. Güntherodt, B. Büchner, T. Lorenz, M. Breuer, J. Zeman, G. Martinez, G. Dhalenne, and A. Revcolevschi, Phys. Rev. B **57**, 7749 (1998).

[55] B. Büchner, U. Ammerahl, T. Lorenz, W. Brenig, G. Dhalenne, and A. Revcolevschi, Phys. Rev. Lett. **77**, 1624 (1996).

[56] M. Poirier, R. Beaudry, M. Castonguay, M. L. Plumer, G. Quirion, F. S. Ravazi, G. Dhalenne, and A. Revcolevschi, Phys. Rev. B **52**, R6971 (1995).

[57] M. Saint-Paul, N. Hegman, G. Reminyi, P. Monceau, G. Dhalenne, and A. Revcolevschi, J. Phys.: Condens. Matter **9**, L231 (1997).

[58] P. Fronzes, M. Poirier, A. Revcolevschi, and G. Dhalenne, Phys. Rev. B **55**, 8324 (1997).

[59] M. Hase, Y. Sasago, I. Terasaki, K. Uchinokura, G. Kido, and T. Hamamoto, J. Phys. Soc. Jpn. **65**, 273 (1996).

[60] B. Grenier, L. P. Regnault, J. E. Lorenzo, J. Bossy, J. P. Renard, G. Dhalenne, and A. Revcolevschi, Physica B **234-236**, 534 (1997).

[61] A. Revcolevschi and R. Collongues, C.R. Seances Acad. Sci., Ser. A **266**, 1767 (1969).

[62] A. Revcolevschi and G. Dhalenne, Adv. Mater. **5**, 657 (1993).

[63] M. Weiden, R. Hauptmann, W. Richter, C. Geibel, P. Hellmann, M. Köppen, F. Steglich, M. Fischer, P. Lemmens, G. Güntherodt, A. Krimmel, and G. Nieva, Phys. Rev. B **55**, 15 067 (1997).

[64] M. Hase, I. Terasaki, Y. Sasagi, K. Uchinokura, and H. Obara, Phys. Rev. Lett. **71**, 4059 (1993).

[65] Since this spontaneous strain at low temperature is obtained by integration, it is not strongly affected by possible sample inhomogeneities, leading, e.g., to a broadening of the transition.

[66] A different temperature dependence of ϵ is, however, observed in the dimerized phase at finite fields (Ref. 43).

[67] B. Grenier and L. P. Regnault (private communication).

[68] F. Schönfeld (unpublished); see also H. Yokoyama and Y. Saiga, J. Phys. Soc. Jpn. **66**, 3617 (1997).

[69] The assumption $\langle A^2 \rangle \propto T_{SP}^2$, which can be inferred from earlier treatments of the SPT yielding $|A| \propto \Delta$ (see, e.g., Refs. 33,2), reveals a much worse description of the data than the cubic dependence shown by the solid line in Fig. 4.

[70] The additional broadening of $\Delta\alpha$ does not depend on the field orientation, i.e., for $H \| c$ it is also found for $H \gtrsim H_{D/I}$.

[71] A. K. Hassan, L. A. Pardi, G. B. Martins, G. Cao, and L-C. Brunel, Phys. Rev. Lett. **80**, 1984 (1998).

[72] L. N. Bulaevskii, A. V. Zvarykina, Y. S. Karimov, R. B. Lyubovskii, and I. F. Shchegolev, Sov. Phys. JETP **35**, 384 (1972).

[73] S. M. Bhattacharjee, T. Nattermann, and C. Ronnewinkel, Phys. Rev. B **58**, 2658 (1998).

[74] M. Fujita and K. Machida, J. Phys. Soc. Jpn. **53**, 4395 (1984).

[75] H. Ohta, S. Imagawa, H. Ushiroyama, M. Motokawa, O. Fujita, and J. Akimitsu, J. Phys. Soc. Jpn. **63**, 2870 (1994).

[76] H. Hori, M. Furusawa, T. Takeuchi, S. Sugai, K. Kindo, and A. Yamagishi, J. Phys. Soc. Jpn. **63**, 18 (1994).

[77] K. Takehana, M. Oshikiri, G. Kido, A. Takazawa, M. Sato, K.

Nagasaka, M. Hase, and K. Uchinokura, Physica B **216**, 355 (1996).

[78] D. Bloch, J. Voiron, J. W. Bray, I. S. Jacobs, J. C. Bonner, and J. Kommandeur, Phys. Lett. **82A**, 21 (1981).

[79] D. Bloch, J. Voiron, J. C. Bonner, J. W. Bray, I. S. Jacobs, and L. V. Interrante, Phys. Rev. Lett. **44**, 294 (1980).

[80] W. H. Korving, G. J. Kramer, R. A. Steeman, H. B. Brom, L. J. de Jongh, M. Fujita, and K. Machida, Physica B **145**, 299 (1987).

[81] It is obtained by dividing the field scale of the calculated phase boundary in Ref. 35 by 1.1. This factor is derived when replacing the susceptibility of the U phase underlying the theory of Cross by the exact result for a one-dimensional Heisenberg chain (Ref. 51) at $T/J \simeq 0.1$. This modification of the theoretical phase boundary was suggested by Cross in order to compare the theoretical result with experimental data.

[82] Remarkably, the anisotropy of the anomalies of α due to the direct coupling between lattice strains and the AFM order parameter also correlates with that at T_{SP}. The reason is that both couplings are related to the uniaxial pressure derivatives of the magnetic susceptibility (Ref. 55).

[83] To include the magnetic field in the free energy describing the SPT is obviously complicated due to the qualitative change of this phase transition in a large magnetic field. Even if we restrict to the D phase the expression in Eq. (10) is not sufficient, since the field dependences of the order parameter at $T \simeq T_N \lesssim 5$ K, on the one hand, and T_{SP} on the other hand, markedly differ (Ref. 43).